

QATAR UNIVERSITY

COLLEGE OF ENGINEERING

A NOVEL ELECTROCOAGULATION SYSTEM FOR PRODUCED WATER

TREATMENT

BY

DEINA TAREK ABDELRAZZEK ALY

A Thesis Submitted to  
the Faculty of the College of  
Engineering  
in Partial Fulfillment  
of the Requirements  
for the Degree of

Masters of Science in Environmental Engineering

January 2018

© 2018 Deina Aly. All Rights Reserved.

## COMMITTEE PAGE

The members of the Committee approve the Thesis of Deina Aly defended  
on 19/12/2017.

---

Muftah El-Naas  
Thesis/Dissertation Supervisor

---

Ramzan Kahraman  
Committee Member

---

Chen J. Paul  
Committee Member

Approved:

---

Khalifa Al-Khalifa, Dean, College of Engineering

## **ABSTRACT**

ALY, DEINA, T., Masters : January : [2018], Masters of Science in Environmental Engineering

Title: A NOVEL ELECTROCOAGULATION SYSTEM for PRODUCED WATER TREATMENT

Supervisor of Thesis: Muftah, El-Naas.

Produced water, which is generated from the Oil & Gas industries, is becoming a global concern due to its complex composition and large volumes. This thesis introduces a novel electrocoagulation system for the treatment of produced water and focuses on the optimization of reactor design rather than operating conditions. Electrocoagulation is an effective electrochemical technology for the treatment of different types of contaminated waters. Most of the recent Electrocoagulation research has been focusing on pollutant-specific evaluation without paying attention to cell design and optimization. The main objective of the study, therefore, is to develop and test a new cell design that can mitigate the problems associated with cathode passivation, which is often outlined by several researchers as a major shortcoming of electrocoagulation systems. Several screening experiments were carried out to select the type of metal for the cell electrodes. The performance of the proposed cell design was tested and compared to other setups, where the new design proved to be more effective in terms of treatment efficiency and passivation prevention. Finally, the system was optimized for the treatment of produced water, using statistical analysis, and then operated continuously at the determined optimum conditions. The new cell design was able to achieve high performance in terms of the reduction of the organic contaminants, reaching up to 96.8%, 97.9% and 94.6% for TOC, TPH and O&G, respectively. In conclusion, this thesis paves the way for future research to focus on the

design and optimization of Electrocoagulation reactors. Future work should also consolidate more efforts towards examining the transition from batch to continuous systems and the possibility of scale up for industrial applications.

## DEDICATION

*This thesis is dedicated to my parents, who supported and motivated me in every possible way through the past two years. To my husband, Islam, whose sacrifice and patience made it possible for me to complete this work. And finally, to my beautiful daughter, Salma, who had to spend endless hours away from me. Thank you for voluntarily choosing to be part of this journey.*

## **ACKNOWLEDGMENTS**

The successful completion of this work is attributed to an amazing team who supported me all the way through. First of all, I would like to express my gratitude to Dr. Muftah El-Naas, my supervisor for his guidance and valuable advice. Special thanks goes to Eng. Yehia Sayed from the Engineering workshop at Qatar University for helping me with fabricating my reactor and making it a reality. Words can't describe my appreciation to all the people from the Environmental Science Centre at Qatar University for allowing me to perform all the required analysis; thank you Ms. Hajer Al-Naimi , Mr. Mazen, Mr. Hassan and Ms. Noora. And finally, a big thank you to the amazing team at the Gas Processing Centre who never fail to guide and support me, thank you Dr. Mustafa Nasser, Dr. Abdelbaki Benamor and Mr. Dan.

## TABLE OF CONTENTS

|   |    |
|---|----|
| List of Tables .....  | x  |
| List of Figures .....   | xi |
| Chapter 1: Introduction .....   | 1  |
| Chapter 2: Literature Review .....  | 6  |
| 2.1 Colloidal Particles Stability and Destabilization.....                | 7  |
| 2.2 Theory of Electrocoagulation .....                                    | 13 |
| 2.3 Factors affecting the efficiency of electrocoagulation process .....  | 17 |
| 2.3.1 Electrode arrangement .....   | 17 |
| 2.3.2 Type of power supply .....  | 19 |
| 2.3.3 Current density .....   | 21 |
| 2.3.4 Concentration of anions .....                                       | 22 |
| 2.3.5 Effect of initial pH .....  | 22 |
| 2.3.6 Electrode material .....  | 25 |
| 2.4 Challenges and recent advances in Electrocoagulation technology ..... | 27 |
| 2.4.1 Challenges.....   | 27 |
| 2.4.2 Recent advances.....  | 28 |
| 2.5 Overview of produced water composition .....                          | 39 |
| 2.5.1 Total dissolved solids (TDS).....                                   | 39 |

|                                  |   |    |
|----------------------------------|---|----|
| 2.5.2                            | Total petroleum hydrocarbons .....                                    | 40 |
| 2.5.3                            | Dissolved & dispersed gasses .....                                    | 43 |
| 2.5.4                            | Production chemicals .....  | 43 |
| 2.5.5                            | Produced solids .....   | 44 |
| 2.5.6                            | Heavy metals.....   | 45 |
| 2.5.7                            | Naturally occurring radioactive materials (NORM) .....                | 47 |
| 2.6                              | Environmental regulations for produced water discharge .....          | 48 |
| 2.7                              | Applications of Electrocoagulation for produced water treatment ..... | 50 |
| Chapter 3                        | .....   | 52 |
| 3.1                              | Experimental setup.....   | 52 |
| 3.2                              | Materials and methods .....   | 54 |
| 3.2.1                            | Synthetic produced water preparation.....                             | 54 |
| 3.2.2                            | Experimental analysis .....   | 56 |
| 3.2.3                            | Experimental procedures.....  | 56 |
| Chapter 4: Results & Discussions | .....   | 58 |
| 4.1                              | Selection of electrode material.....                                  | 58 |
| 4.1.1                            | COD results.....  | 58 |
| 4.1.2                            | TOC, O&G and TPH results .....  | 62 |
| 4.1.3                            | Sludge characterization .....   | 63 |
| 4.2                              | Selecting electrode geometry .....                                    | 70 |
| 4.2.1                            | TOC, O&G and TPH results .....  | 70 |



|  |  |     |
|--|--|-----|
| 4.2.2  | Power consumption and potential difference between the electrodes..... | 72  |
| 4.3  | Optimization of selected geometry .....                                | 76  |
| 4.3.1  | Theory and steps of RSM.....   | 76  |
| 4.3.2  | RSM results and discussions.....                                       | 78  |
| 4.4  | Continuous mode of operation.....                                      | 92  |
| Chapter 5: Research findings and conclusions ..... |  | 98  |
| Chapter 6: Future work .....                       |  | 100 |
| References.....                                    |  | 101 |

## List of Tables

|  |    |
|--|----|
| Table 1: Inorganic constituents of oil & gas produced waters (PW) compared to seawater .....   | 40 |
| Table 2: Concentrations of typical production chemicals in oil and gas produced waters .....   | 44 |
| Table 3: Concentration of heavy metals in oil and gas produced waters, adapted from [98] ..... | 46 |
| Table 4: Typical activities of radium isotopes in produced water and sea water [3] .....       | 47 |
| Table 5: Maximum allowable O&G limit for PW discharge according to regional conventions..      | 50 |
| Table 6: Applications of EC for produced water treatment .....                                 | 51 |
| Table 7: Characteristics of synthetic produced water .....                                     | 55 |
| Table 8: COD results using high range vials .....  | 59 |
| Table 9: COD results using low range vials .....   | 60 |
| Table 10: Chloride cuvette test results .....  | 61 |
| Table 11: Performance comparison of aluminum and iron electrodes .....                         | 62 |
| Table 12: Performance comparison of different electrode geometries .....                       | 70 |
| Table 13 : Power consumption and potential difference for different electrode geometries ..... | 73 |
| Table 14: Maximum and minimum levels of experimental factors .....                             | 79 |
| Table 15: Summary of experimental design and responses .....                                   | 80 |
| Table 16: TOC response and optimum conditions, first scenario .....                            | 86 |
| Table 17: TOC, TPH and O&G responses and optimum conditions for second scenario .....          | 87 |
| Table 18: Predicted response versus experimental response at optimum conditions .....          | 91 |
| Table 19: TOC removal percent, potential difference and power consumption versus time .....    | 93 |
| Table 20: Summary of TOC, TPH and O&G removal after continuous operation .....                 | 97 |

## List of Figures

|  |    |
|--|----|
| Figure 1: Electric double layer illustration .....   | 8  |
| Figure 2: DLVO theory illustration .....   | 10 |
| Figure 3: Electrocoagulation cell [2] .....  | 14 |
| Figure 4: E-pH diagram of iron at 25 ° C.....  | 16 |
| Figure 5: E-pH diagram for Aluminum at 25 ° C.....   | 17 |
| Figure 6: Types of electrode configurations [2].....   | 21 |
| Figure 7: Classification of hydrocarbons [1] .....   | 42 |
| Figure 8: Illustration of batch EC setup .....   | 53 |
| Figure 9: Illustration of continuous setup .....   | 53 |
| Figure 10: Electrode configurations and dimensions.....  | 54 |
| Figure 11: A schematic diagram of the experimental steps .....   | 58 |
| Figure 12: Performance of aluminum and iron plate electrodes .....   | 63 |
| Figure 13: Aluminum sludge .....   | 64 |
| Figure 14: Iron sludge.....  | 65 |
| Figure 15: Al Sludge characterization using XRD .....  | 66 |
| Figure 16: Comparison between aluminum and iron floc size .....  | 67 |
| Figure 17: FE Sludge characterization using XRD.....   | 69 |
| Figure 18: TOC, TPH and O&G reduction with five different aluminum electrode geometries... 71                            |    |
| Figure 19: Initial and final potential difference for different electrode geometries. PD is potential difference.....    | 74 |
| Figure 20: Power consumption for different electrode geometries at constant current of 1,3 A. ... 75                     |    |
| Figure 21: Cathode passivation with different electrode geometries: a (Al-Plate), b( Al-NPR), c(Al-PR), d(Al-PR-C) ..... | 76 |

|  |    |
|--|----|
| Figure 22: Untreated sample (left) and treated sample (right) at pH 10 .....                   | 82 |
| Figure 23: XRD results for PW sludge at pH 10 .....  | 85 |
| Figure 24: Surface plot of TOC versus CD and AF at pH of 7.....                                | 86 |
| Figure 25: Surface plots for TOC response .....  | 89 |
| Figure 26: Surface plots for O&G response.....   | 88 |
| Figure 27: Surface plots for TPH response .....  | 90 |
| Figure 28: Optimum conditions for second scenario .....  | 91 |
| Figure 29: TOC reduction percent versus time for continuous operation.....                     | 94 |
| Figure 30: Potential difference and power consumption versus time for continuous operation.... | 95 |
| Figure 31: Cathode passivation after 90 minutes of continuous operation.....                   | 96 |

**Parts of this thesis have already been published as:**

D. T. Moussa, M. H. El-Naas, M. Nasser, and M. J. Al-Marri, "A comprehensive review of electrocoagulation for water treatment: Potentials and challenges," *Journal of Environmental Management*, vol. 186, Part 1, pp. 24-41, 1/15/ 2017.

D. T. Moussa, M. H. El-Naas , Electrochemical technologies for produced water treatment, Chapter 13 in *Inorganic Pollutants in Wastewater: Methods of Analysis, Removal and Treatment*, Editors: Inamuddin, Abdullah M. Asiri and Ali Mohammad, Materials Research Forum (2017). ISBN 978-1-945291-34-0.

## **Chapter 1: Introduction**

During the production operations of oil and gas, a process known as hydraulic fracturing is employed, where large volumes of water is injected at high pressure to stimulate the formation. When such injected water is extracted along with the oil and gas, it is usually highly contaminated with hydrocarbons, solids, gases and other impurities. Besides injected water, naturally occurring water in the reservoir formation within the pores of the rocks (formation water), is also extracted. Formation water together with injection water are collectively known as produced water, a term that gained considerable attention in recent years. The volume of produced water generally increases as the production of oil & gas decreases; new oil and gas wells produce less water than depleted wells [3]. The water to oil ratio (WOR) or water to gas ratio (WGR) could be as low as zero for new wells and as high as 50 for depleted wells [4]. Once the cost of treating and disposing produced water exceeds the profit of selling the extracted oil and gas, the well is shut in. Produced water is often identified as a waste or byproduct of the oil and gas industry; thus, the effort to recycle and reuse produced water is minimal. The most common way of disposing produced water is through deep underground injection in porous formation; however, this method has raised concerns about the quality of underground drinking water [5].

Almeida et al. reported that by 2030, oil will account for 32% of the global energy supply with the oil demand rising to 107 million barrels per day (mbpd) compared to 85 mbpd back in 2006 [6]. This means that oil related effluents, specifically produced water that accounts for more than 80% of liquid waste, would be generated at larger volumes.

According to Duraisamy et al., the volume of produced water extracted along with oil and gas exceeds 77 billion bbl per year globally [7]. Oilfields alone account for more than 60% of the total volume of produced water globally [8].

According to an article published by the world resources institute, the gulf region suffers from an extremely high water stress [9]. Water stress is defined as the ratio of water withdrawal to water supply which is given a value of  $>80\%$  for the gulf region. These countries are also known to be major oil & gas producers, and hence are producers of large volumes of produced water. It is also worth mentioning that this area lacks the presence of natural fresh water resources other than ground water, which is becoming increasingly saline due to seawater intrusions. The large volumes of produced water can be treated and utilized to replenish the freshwater supply that is becoming increasingly scarce, making the potential reuse of treated produced water an attractive opportunity. Treated produced water could be used in various applications such as irrigation for landscaping or food crops, fire control, cooling water for chemical processes, wildlife-livestock, dust control and vehicle/ equipment washing which in turn would reduce freshwater consumption [5, 10-15].

Conventional produced water treatment technologies can be categorized into three major groups: physical, chemical, and biological processes. A typical produced water treatment process consists of a combination of physical, chemical, and biological unit operations to target the removal of different constituents/ pollutants. Physical unit operations depend purely on the physical separation of pollutants from wastewater without causing a significant change in the chemical or biological characteristics of the treated water [2]. Chemical processes are referred to as additive processes since they require the

addition of chemicals to react with the contaminants and achieve the desired removal. The additive nature of chemical processes makes them less favorable compared to other processes. Biological unit processes utilize microorganisms for the biodegradation of contaminants in wastewater, and the main aim of these processes is to reduce the organic content and nutrients in wastewater. Biological units are generally classified into aerobic, anaerobic or facultative depending on the availability of dissolved oxygen in wastewater [16].

Although the above mentioned technologies effectively eliminate most of produced water contaminants, they have limited efficiencies when dealing with small droplets of suspended oils and/ or dissolved contaminants. Moreover, each of the above- mentioned processes has its own limitations; physical processes normally require large surface area, huge capital cost and in the case of an adsorptive physical process, the regeneration of adsorbent is quite expensive. Chemical additives, on the other hand, require the addition of chemicals causing an increase in the net dissolved constituents in wastewater and rendering it impractical to reuse in other applications. This mechanism also generates hazardous sludge and could have high operational cost. Biological processes are not yet practical for handling produced water as the microorganisms are very sensitive to the inlet feed concentration and salinity, a major problem in produced water [17].

Due to the wide variation in produced water composition, quality, and volume throughout the lifetime of the oil/gas well, a robust technology that could adapt to the varying operating conditions in produced water is required. Other than the above-mentioned processes, promising and relatively new technologies that utilize the concepts of electrochemistry are also available. Examples of electrochemical water treatment



technologies include Electrocoagulation, Electrodialysis, Electro-oxidation, Electrodeionization and capacitive deionization. Although using electricity for water treatment applications goes back to the 18<sup>th</sup> century, they were found impractical due to the high capital and electricity cost required [18, 19]. However, during the past two decades, electrochemical wastewater treatment technologies started to regain importance as an environmentally friendly option that generates minimal sludge, requires no chemical additives and requires minimal footprint without compromising the quality of the treated water.

Despite the wide range of electrochemical wastewater treatment technologies, they are all based on the electrolysis process. A typical electrochemical cell consists of two metal electrodes connected to an external power source that supplies electric current. The metal electrodes are immersed in the electrolytic solution, which is the wastewater in case of wastewater treatment. The efficiency of the electrochemical cell is greatly affected by the conductivity of the electrolytic solution as the presence of dissolved ions enhances performance of the electrochemical cell. The extreme salinity of produced water favors the electrochemical reaction as the conductivity is high.

This thesis focuses on Electrocoagulation (EC) technology for the treatment of produced water. Electrocoagulation is an advanced technology that combines the benefits of electrochemistry, coagulation and flotation [2, 20, 21]. Although each of the three techniques have been studied extensively on a separate manner, there is limited literature available on integrating these three technologies which forms the basis of electrocoagulation. During the past decade, vast amount of research has been devoted to utilizing electrocoagulation for the treatment of several types of wastewater, ranging from

groundwater to highly contaminated refinery wastewater. However, most of the recent EC research has been focusing on pollutant-specific evaluation without paying attention to cell design and optimization. This thesis introduces a novel EC system for produced water treatment. The scope of this thesis focuses on optimization of reactor design rather than operating conditions, therefore, overcoming the existing gap in EC research. The cell design aims at solving problems like cathode passivation and electrode deterioration which are outlined by several authors in the literature as major EC shortcomings. In the following chapter, an extensive review of EC theory, applications, challenges and improvements as well as a detailed characterization of produced water will be presented.

## **Chapter 2: Literature Review**

As mentioned previously, EC technology combines the benefits of coagulation, floatation and electrochemistry. The theory behind chemical coagulation /flocculation (CC/CF) and EC is basically the same. Both methods target the removal of particles from wastewater through destabilizing/neutralizing the repulsive forces that keep the particles suspended in water. When the repulsive forces are neutralized, the suspended particles will form larger particles that can settle down for easier separation from water. The main advantage of EC over CC/CF is that CC/CF uses chemical coagulants/flocculants such as metal salts or polyelectrolytes while in EC the coagulants are generated in situ by the electrolytic oxidation of an appropriate anode material, which results in much less sludge generation [22]. Another major advantage of EC over CC/CF and other conventional water treatment methods is the potential of treating oily water, where the presence of electric current can contribute to the electrocoalescence of oil droplets. Electrocoalescence has been proven effective in dealing with tight emulsions, where the droplets are very small [23]. Very tight emulsions are often encountered in the Oil and Gas industry, either through the presence of fine water droplets in oil or vice versa, as is the case in produced water. Prior to exploring the theory of EC, it is important to look at the colloidal system properties and stability.

## **2.1 Colloidal Particles Stability and Destabilization**

Colloidal particles exist in many natural and engineered systems. Colloidal particles stability is often explained by the presence of repulsive electrical charges on the surface of particles and stability can be estimated by considering the interaction forces between the particles. When repulsive forces are dominant, the system will remain in a dispersed state. In contrast, when the interaction forces control, the particles will coagulate/flocculate and the suspensions maybe destabilized. Particles with the same charge repel each other, therefore, this repulsion needs to be minimized if destabilization is required. Colloids are microscopic particles that are typically in the range of 1 nm to 2 $\mu$ m, resulting in a very small ratio of mass to surface area. Given that their total surface area is large compared to their mass and size, the gravitational forces of colloids are often neglected as compared to the surface phenomena predominating when studying colloidal suspension [24]. In order to neutralize the charge, counter charged particles are used to be attracted to the surface of the colloids forming an electric double layer as illustrated in Figure 2.

The electric double layer consists of an inner region (stern layer), where oppositely charged ions are tightly bound to the surface of colloidal particles and an outer layer, where the ions move freely due to diffusion (Ion diffuse layer or slipping plane). The interface of the inner and outer layers is known as the shear surface which defines the outer limit of the stern layer [25]

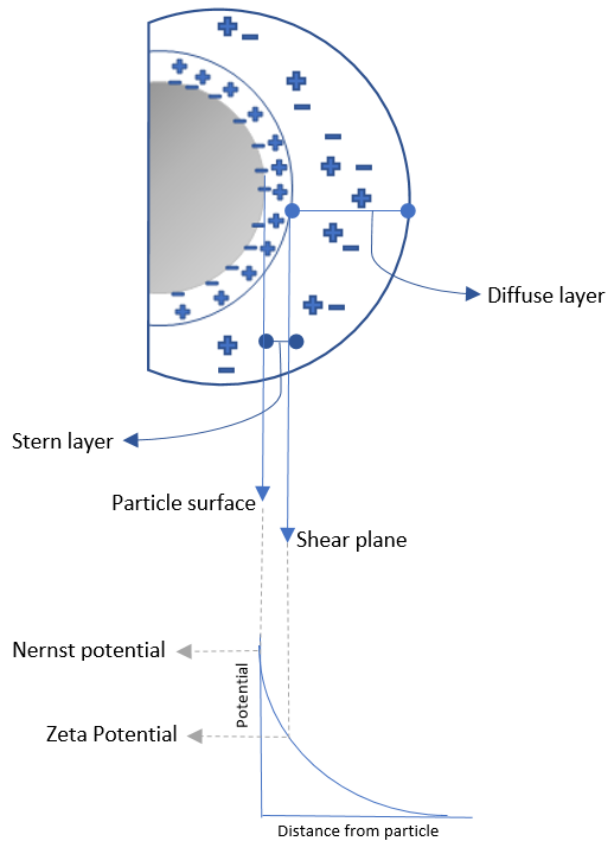


*Figure 1: Electric double layer illustration*

The maximum potential occurs at the surface of colloidal particle and is known as the Nernst potential, where it decreases across the stern layer due to the presence of oppositely charged particles resulting in what is defined as the Zeta potential measured at the surface of shear (Figure 1) [24, 25]. Zeta potential is the main reason of colloidal system stability, as it represents the electrical charge difference between the first and second layers and gives an indication of the extent of repulsion between colloidal particles carrying the same

charge. The higher the value of Zeta potential, the greater the magnitude of repulsion between particles and consequently, the more stable is the colloidal system. In general, colloidal particles in suspensions with zeta potentials more positive than +30 mV or more negative than -30 mV are normally considered stable [26].

DLVO (Derjaguin-Landua- Verwey-Overbeek) theory is a good starting point to describe the stability of colloidal particles [27-31]. Simply, DLVO theory considers the contributions of the attractive van der Waals potential and the repulsive electrostatic potential. Therefore, according to DLVO theory, the dispersed particles are under the effect of two independent forces: attractive van der Waals force and the repulsive electrostatic force arising from the presence of electrical double-layer at particles surfaces. The charges on the particles will be balanced by equal and opposite ions solution. This means that there will be an excess of positive charge accumulated in the interfacial region around a negative ion, and this will govern the electrostatic effects [27]. This is called electrical-double layer and is shown in Figure 1. It follows that the electrostatic double-layer interaction ( $V_t$ ) between two particles is the outcome of the overlap of two double layers.

According to DLVO theory, the net interaction energy ( $V_t$ ) of two particles is given by the sum of Van der Waals attraction energy ( $V_A$ ) and electrostatic repulsion energy ( $V_R$ ), as presented in Figure 2 as a function of the distance ( $X$ ) between two particles. The attractive energy of interaction ( $V_A$ ) is inversely proportional to  $X$  and hence increases rapidly as the oil droplets approach each other. Contrarily, the repulsive energy ( $V_R$ ) depends exponentially on  $X$  and changes more slowly. The net interaction curve ( $V_A + V_R$ ) in Figure 2 shows three distinct features: a primary minimum, a secondary minimum and a maximum [32, 33].

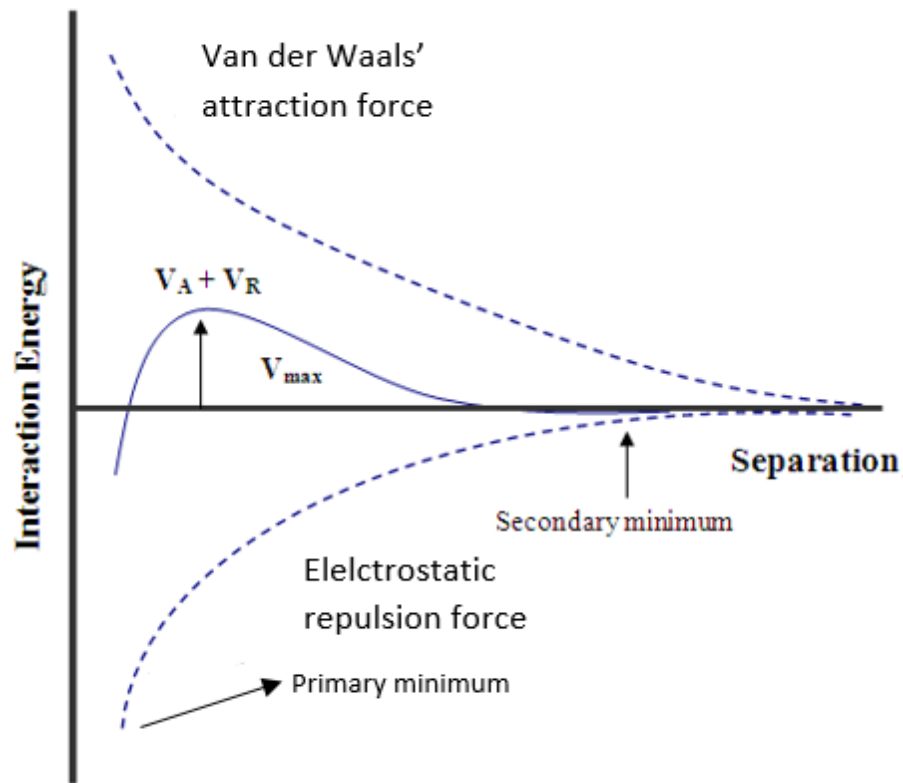


Figure 2: DLVO theory illustration

As mentioned earlier, the role of coagulants/flocculants in either CC/CF or EC is to destabilize the colloids by reducing the repulsive forces and forcing the particles to agglomerate for easier separation. Coagulation/flocculation follows four different mechanisms to destabilize colloidal systems depending on several factors such as chemical and physical properties of the solution, coagulant/flocculant and pollutant types. These mechanisms are briefly summarized below.

## **1- Compression of the electrical double layer :**

The thickness of the electric double layer affects the extent of repulsion between particles and hence their stability. As the thickness of the double layer decreases, the repulsive forces are also reduced and particles can easily come together forming larger particles. In order to compress the electrical double layer, counter charged ions are added to the solution either by metal salts/electrolytes in case of CC/CF or by oxidation of the anode in case of EC. In both cases, these metal ions will diffuse through the double layer causing higher counter ion concentration around the colloidal particle, which in turn reduces the electrical double layer thickness and repulsive forces. When the electrical double layer thickness is compressed, the Zeta potential measured at the shear surface will also be reduced and the optimum destabilization happens if Zeta potential approaches 0 mV.

When added to the solution, different metal ions have different destabilization ability. This is best explained by looking at Schultze-Hardly rule, which simply states that as the charge of added counter metal ions increases, its ability to destabilize the colloidal particles also increases. Therefore, it is favorable to use divalent or trivalent metal ions to destabilize counter charged colloids. It is worth mentioning that this mechanism is characterized by large metal ions concentration to achieve destabilization, which makes it impractical for water treatment [24, 25, 34].

## **2- Adsorption/ charge neutralization:**

The concept of this destabilization mechanism is quite simple, where adsorption of counter charged ions on the surface of colloidal particles results in neutralizing their



surface charge so that repulsive forces are overcome and van der Waals attractive forces dominate. Eventually colloidal particles approach each other and coagulate [24, 25, 34].

### **3- Adsorption/ inter-particle bridging:**

When metal coagulants are polymerized, they have the ability to form links/ bridges between colloidal particles especially when the polymers have high molecular weight and long chain. This phenomena is due to the reactive groups that polymers have which can adsorb to the colloids surface in various forms including: charge- charge interactions and hydrogen bonding. The bridging of colloidal particles results in the formation of bigger particles and hence destabilization. This mechanism is quite risky, since colloidal particles can be restabilized in cases where the polymer's chains are attached to all colloidal particles existing, but there are some free extended chains not attached to any particles. In such circumstances, the free chain will reattach to the same particle and cause destabilization. It is therefore crucial not to use an overdose of polymers. In addition to overdosing of polymer, rapid mixing could also break the bridging between colloids and eventually restabilize them [24, 25].

### **4- Entrapment of particles in precipitate:**

This mechanism, also called sweep coagulation, is often encountered when high metal salt concentrations are added. In such cases, the metal salts react with water forming insoluble metal hydrates that precipitate forming a sludge blanket. The formed precipitates eventually entrap colloidal particles during and after precipitation [24, 25].

## 2.2 Theory of Electrocoagulation

After understanding the stabilization and destabilization of colloidal systems, it is time to explore the theory of electrocoagulation, which is an advanced technology combining coagulation, flotation and electrochemistry. Each of the three technologies has been studied extensively in a separate manner; however, there is limited literature available on integrating these three technologies that are the basis of EC. The complexity of EC technology is also attributed to the fact that it utilizes several pollutant removal mechanisms including sweep coagulation, floatation and adsorption. The pollutant removal mechanism is determined by the nature of coagulants generated in the solution as well as the properties of dissolved ions and contaminants in wastewater. Although several researchers have reported the effectiveness of EC to treat a wide range of pollutants, they weren't able to explain the theory behind it [22]. The literature indicates that the history of EC extends to the past hundred years, where it has been employed to treat water containing pollutants such as: heavy metals, tannery, textile and colored wastewater, pulp and paper industry wastewater, oily wastewater and food industry [20, 35]. A review of the applications of EC is discussed in details in section 2.7.

The basic EC unit typically consists of an electrolytic cell with an anode and cathode metal electrodes connected externally to a DC power source and immersed in the solution to be treated as shown in Figure 3. Iron and aluminum electrodes are the most extensively used metals for EC cells since these metals are available, non-toxic and proven to be reliable. Although EC is considered to be quite similar to CC/CF in terms of the destabilization mechanism, it still differs from CC/CF in other aspects such as the side reactions occurring simultaneously at both electrodes. The anode serves as the coagulant in an EC cell, where

it dissociates to give metal cations when current passes through the cell. The dissociation of anode follows Faraday's law given by:

$$m = \frac{ItM_w}{zF} \quad (1)$$

where  $I$  is the current (A),  $t$  is the time of operation (s),  $M_w$  is the molecular weight (g/mol),  $F$  is Faraday's constant (96485 C/mol),  $z$  is the number of electrons involved in the reaction and  $m$  is the mass of anode dissolved (g).

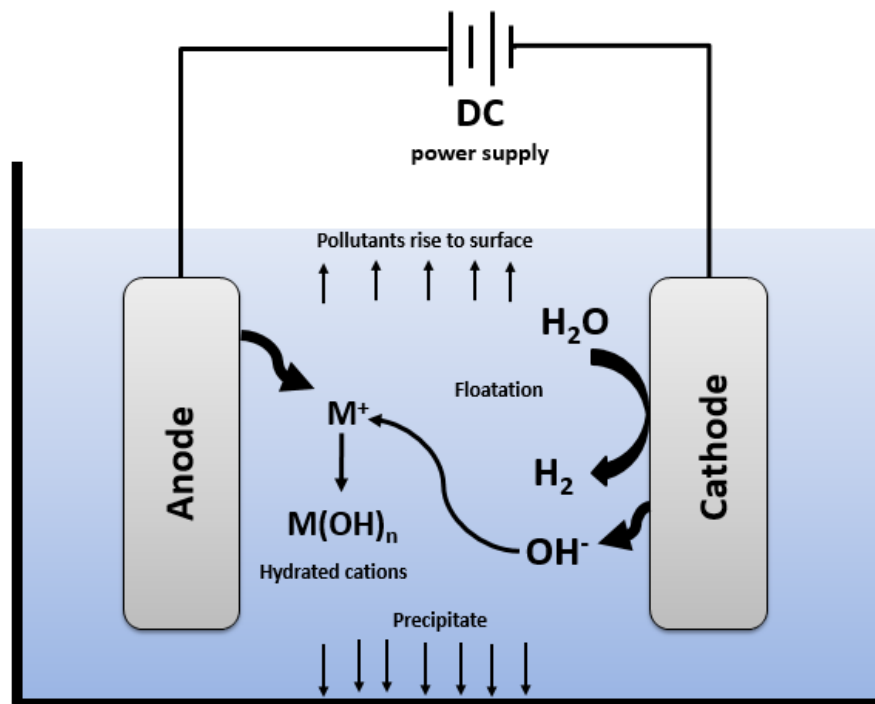
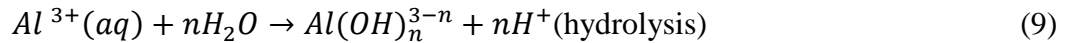
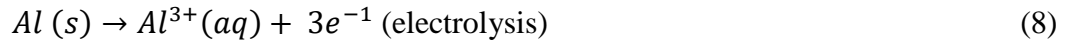
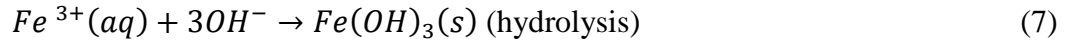
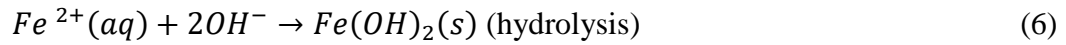
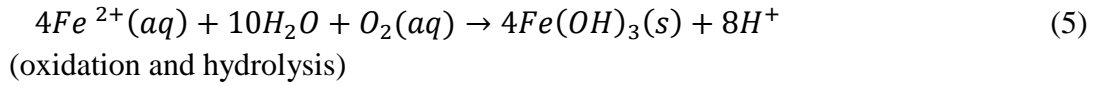
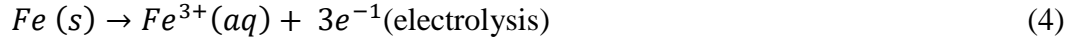
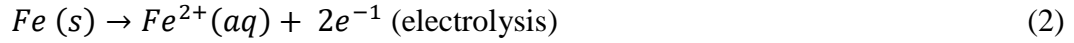


Figure 3: Electrocoagulation cell [2]

All the possible anodic reactions reported in literature, are expressed by Eqs. (2-9) for both aluminum and iron electrodes.



Theoretically, iron anodes may dissociate into divalent or trivalent ions, depending on the pH of the solution and the potential, as illustrated in Eqs. (2-4). On the other hand, aluminum only dissolves as trivalent cations. Using the E-pH diagram for iron & aluminum (Figure 4&5), the stable compounds at a specific pH and potential could be predicted. Several factors control the electrochemical reactions and the generated coagulant species in an EC cell including pH, dissolved oxygen and cell potential, this will be discussed in a separate section.

As mentioned previously, several side reactions occur in the EC cell, which includes evolution of hydrogen bubbles at the cathode along with OH<sup>-</sup> ions, where it causes an increase in pH of the solution as expressed by Eq. 7:



In some cases, the actual anode dissolution does not match the one calculated using

Faraday's law, which indicates that other electrochemical reactions might be taking place at the anode. Several authors suggested that evolution of oxygen at the anode might take place at alkaline pH and sufficiently high anodic potential (Eq. 8) which might be the reason behind the mismatch of theoretical and actual anodic dissolution [18, 25, 34, 36-38].

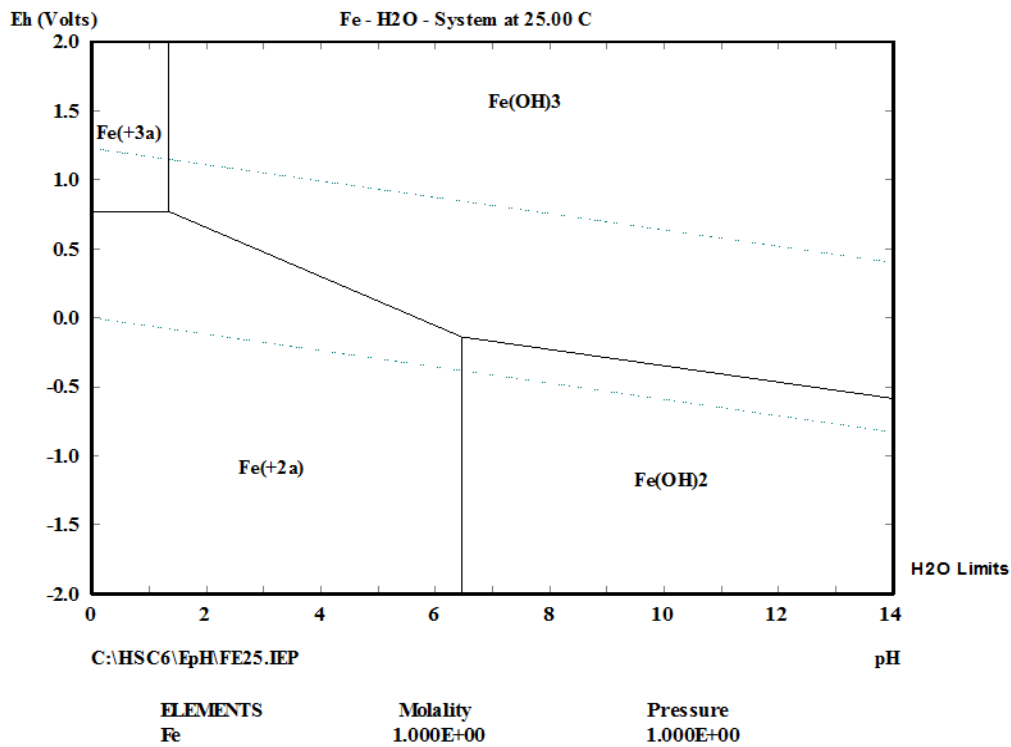


Figure 4: E-pH diagram of iron at 25 °C

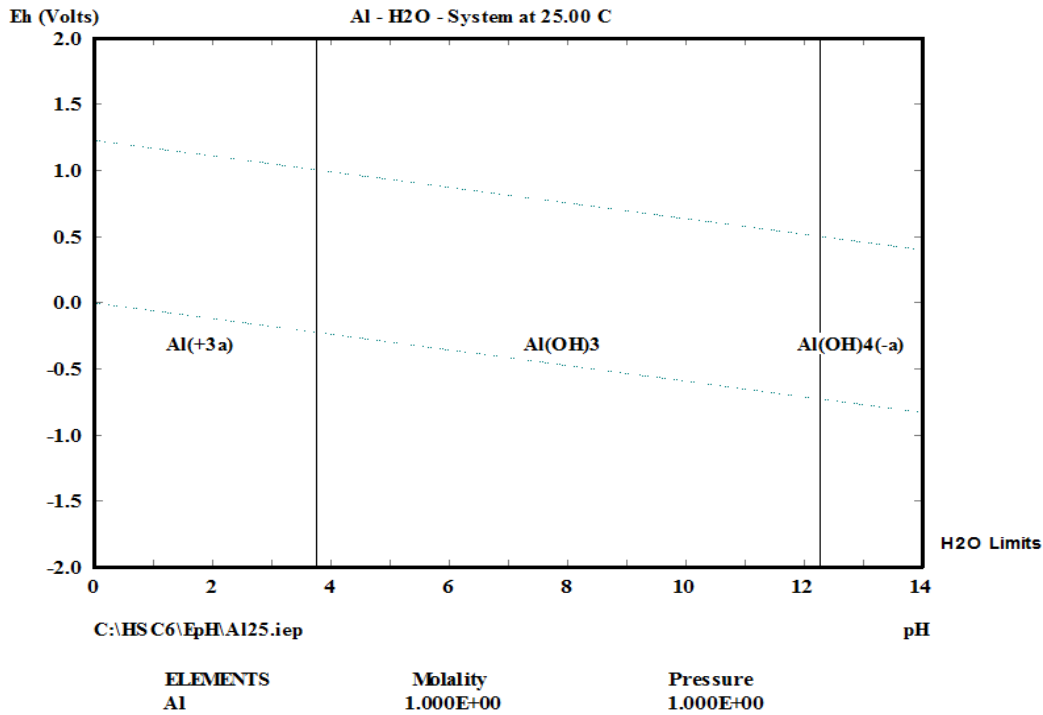


Figure 5: E-pH diagram for Aluminum at 25 °C

### 2.3 Factors affecting the efficiency of electrocoagulation process

Several parameters are known to have an influence on electrocoagulation efficiency and its ability to remove pollutants from wastewater; the most important parameters are discussed in this section:

#### 2.3.1 Electrode arrangement

Regardless of the simplicity of the basic EC setup illustrated in Figure 3, it is not suitable for practical wastewater treatment applications as it requires huge surface area of the electrodes, this is overcome by using monopolar or dipolar electrode

setups in series or parallel connections as illustrated in Figure 6.

In monopolar- parallel (MP-P) configuration, all the anodes are connected to each other and to the external DC supply, and the same thing applies to cathode electrodes. In this configuration, the current is divided between the electrodes resulting in a lower potential difference if compared to the electrodes connected in series. On the other hand, monopolar- series (MP-S) connection is achieved when the two outermost electrodes are connected to the external circuit forming the anode and cathode while each pair of the inner electrodes are connected to each other without an interconnection to the outer electrodes. In this case, the cell voltage is added giving a higher potential difference. The inner electrodes are known as the “sacrificial electrodes” that could be made of similar or different metals and their role is to reduce the consumption of the anode and passivation of the cathode.

The third option is the bipolar- series (BP-S) configuration in which the outermost electrodes are directly connected to the external power supply with the inner electrodes not connected by any means. Once current passes through the main electrodes, the adjacent side of inner electrodes gets polarized and will carry a charge opposite to the charge of the nearby electrode. In such configuration, the two outermost electrodes are known to be monopolar while the inner sacrificial electrodes are bipolar. [25, 34, 39-42].

The choice of the appropriate electrode connection mode is determined by the removal efficiency and treatment cost and has been investigated in several studies. Demirci et al. [41] studied the effect of different electrode connections (MP-P, MP-S, BP-P) on the color, turbidity removal and total treatment cost of EC of textile

wastewater treatment. His results proved that the removal efficiencies were similar for all three connections; however, the MP-P configuration is the most cost effective. Kobya & Demirbas [40] proved the same results, where MP-P mode gave the highest removal efficiencies and lowest operating cost for EC treatment of can manufacturing wastewater. In an experiment to remove  $\text{Cr}^{3+}$  from aqueous solutions using EC with mild steel electrodes, Golder et al. [43] studied the effect of monopolar and bipolar connections on the current efficiency,  $\text{Cr}^{3+}$  removal and operating cost. The results showed that monopolar connection gave much higher current efficiency with lower operating cost compared to bipolar connection. However, bipolar connection resulted in an almost complete removal of  $\text{Cr}^{3+}$  compared to 81.5% with monopolar connection. The removal of fluoride from drinking water was better when bipolar electrodes were used but the total operating cost of monopolar electrodes was much less as reported by Ghosh et al. [44]

### **2.3.2 *Type of power supply***

DC power supply is typically used for electrocoagulation cells; however, after some time of operation, using DC leads to oxidation/ consumption of the anode and a formation of an oxide layer on the cathode known as cathode passivation. Passivation causes an increase in passive over potential, which leads to higher power consumption; the passive layer also results in a decreased flow of current between the two electrodes and decreases the efficiency of EC. Yang et al. [45] highlighted that passivation problem could be cured by adding a sufficient amount of chloride ions which breakdown the passive layer or by applying an alternating



pulsed current (APC) which prevents the formation of passive layer when Al or Fe electrodes are used.

Several studies have reported promising results using AC power supply. Mollah et al. [39] reported that AC ensures reasonable electrode life due to the cyclic energization which delays the traditional electrode consumption encountered in DC. Vasudevan et al. [46] studied the effect of AC & DC on the removal of cadmium from water using electrocoagulation and the results proved that lower energy consumption & higher pollutant removal efficiency is achieved using AC power supply. In a study of the effect of alternating current EC on dye removal from aqueous solutions, Eyvas et al. [47] proved that a higher removal efficiency in shorter operation time is achieved when using APC; moreover, the removal efficiency didn't decrease with time as in the case of DC. They also reported that the operating cost of APC is much less than DC system which makes it more economical.

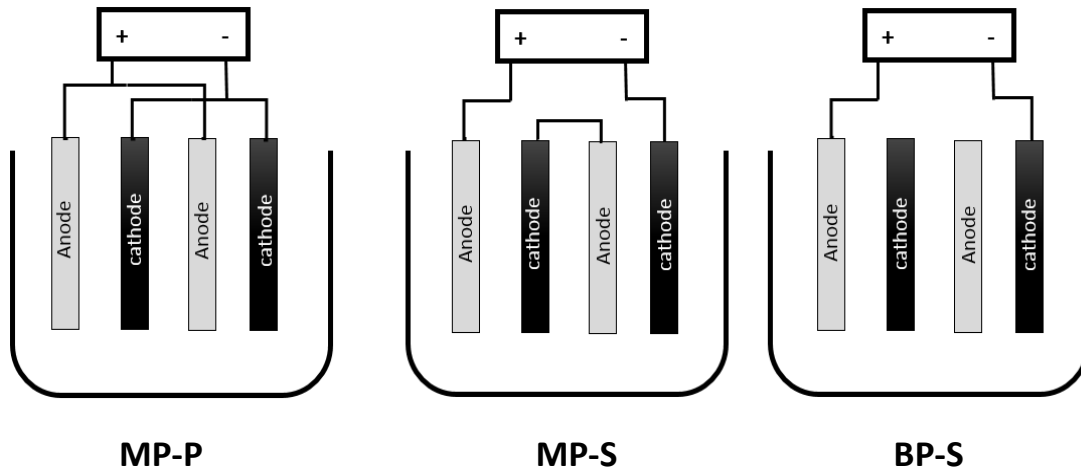


Figure 6: Types of electrode configurations [2]

### 2.3.3 Current density

Current density, which is the current per area of electrode, determines the amount of metal ions released from the electrodes. In general, metal ion dissociation is directly proportional to the applied current density. However, when too large current is used there is high chance of wasting electrical energy in heating the water and even a decrease in current efficiency expressed as the ratio of the current consumed to produce a certain product to the total current consumption. The current density also determines the size of gas bubbles generated whether from the anode or the cathode which in turn, affects the efficiency of the process. There is a critical value for current density which if exceeded the quality of treated water does not show significant improvement. The selection of an optimum value for current density is also affected by other parameters such as pH, temperature and water

flowrate [18, 42]. Several researchers studied the effect of current density on the operation/ efficiency of EC at different operating conditions [36, 48-53].

#### ***2.3.4 Concentration of anions***

The presence of different anions has different effects on the destabilization properties of metal ions. Sulfate ions are known to inhibit the corrosion/ metal dissolution from the electrodes and hence they decrease the destabilization of colloids and reduces current efficiency by increasing the potential between the electrodes. On the other hand, chloride and nitrate ions prevent the inhibition of sulfate ions by breaking down the passive layer [25, 42, 54, 55].

The conductivity of the solution is an important factor that affects the efficiency and power consumption of EC, the higher the conductivity, the lower the power consumption of EC due to the increased pollutant removal efficiency. Therefore, the conductivity of the solution is enhanced by adding anions in the form of salts such as NaCl. It was also found that the presence of chlorine ions effectively contributes to water disinfection [18, 42].

#### ***2.3.5 Effect of initial pH***

pH is a key parameter when it comes to electrocoagulation as it affects the conductivity of the solution, zeta potential and electrode dissolution. It is however difficult to establish a clear relationship between the pH of the solution and the efficiency of electrocoagulation since pH of the treated water changes during EC process, therefore it is usually referred to the initial solution pH [18, 24, 25, 48, 50]. Aluminum and iron anodes behave in a different manner during EC as discussed

below:

#### **2.3.5.1 Aluminum anodes**

As mentioned previously, when aluminum is used as the anode, it undergoes electrolysis according to Eq. 8 to form trivalent aluminum ions, which is followed by spontaneous hydrolysis according to Eq. 9 to give various species depending on the pH of the solution. The anodic reactions make the vicinity of the anode slightly acidic, which is opposed, by the cathode vicinity being slightly alkaline due to hydrogen evolution and production of OH<sup>-</sup> ions. As a general observation, when the initial pH of the solution is highly acidic (pH < 3) or highly alkaline (pH > 11) there is no considerable change in the initial pH. However, when the initial pH is acidic, pH is expected to rise throughout the EC process and when the initial pH is alkaline, pH is expected to decrease along the EC process. Hence, EC using aluminum anode is considered a pH neutralizer [18, 36, 56, 57].

Barrera- Diaz et al. studied the predominant aluminum species present in the solution at different pH values, where they found that at pH less than 3.5, Al<sup>3+</sup> is the major specie present, for pH values between 4 and 9.5, Al(OH)<sub>3</sub>(S) predominates and when the pH is greater than 10, Al(OH)<sub>4</sub><sup>-</sup> forms. The same results could be found using the E-pH diagram for aluminum (Figure 5), as it gives the thermodynamically stable aluminum species at a given pH and cell potential. Barrera-Diaz et al. [58] also investigated the effect of initial pH on the reduction of COD and found that the best removal efficiency is achieved within the pH range of 6-8 and the least removal efficiency occurred at a highly alkaline pH of 12. These

results are quite reasonable since  $\text{Al(OH)}_3(\text{S})$  traps the colloids/ pollutants in a sweep coagulation manner as it precipitates. On the other hand,  $\text{Al(OH)}_4^-$  is known to be a very soluble weak coagulant as it carries a negative charge and will not be able to destabilize colloids [59-61]. Several authors reached the same conclusion that the maximum performance of EC using aluminum anodes is around neutral pH [36, 37, 59, 61-64].

#### 2.3.5.2 *Iron anodes*

Unlike aluminum anodes, iron can dissolve as divalent or trivalent cations, which are then hydrolyzed to form insoluble iron compounds depending on the pH of the solution and the cell potential (Eq. 2-7). The electrochemical dissolution mechanism of iron anodes reported in the literature is not consistent and lack an experimental proof of the actual species formed during EC. Several authors reported the formation of  $\text{Fe}^{2+}$  as a result of electrolysis followed by hydrolysis to produce  $\text{Fe(OH)}_{2(\text{S})}$  [35, 39, 65-67]; others reported further oxidation of  $\text{Fe}^{2+}$  and then hydrolysis to form  $\text{Fe(OH)}_{3(\text{S})}$  [39, 57, 67]. Few authors reported direct electrolysis of iron to form  $\text{Fe}^{3+}$  followed by hydrolysis to give  $\text{Fe(OH)}_{3(\text{S})}$  [34, 66]. Clifford et al.[68] performed an experimental analysis of the species formed during iron electrocoagulation at different pH ranges to validate the findings reported in the literature. The results revealed that iron electrolysis leads to the formation of  $\text{Fe}^{2+}$  which then undergoes oxidation in presence of dissolved oxygen and suitable pH to form  $\text{Fe}^{3+}$  that is finally hydrolyzed to form insoluble  $\text{Fe(OH)}_{3(\text{S})}$ /  $\text{FeOOH}_{(\text{S})}$ . During EC, the production of  $\text{OH}^-$  ions at the cathode temporally elevates the pH

before it gets consumed by the  $\text{Fe}^{2+}$  generated at the anode, which speeds up the rate of  $\text{Fe}^{2+}$  oxidation to  $\text{Fe}^{3+}$ . pH then decreases as  $\text{OH}^-$  ions are consumed at the anode. It was also found that at relatively low pH (6.5 to 7.5) the rate of  $\text{Fe}^{2+}$  oxidation and hydrolysis is slow which results in an increase in the solution pH and formation of a mixture of soluble ferrous ions and insoluble  $\text{Fe}(\text{OH})_{3(\text{s})}/\text{FeOOH}_{(\text{s})}$ . When the pH becomes alkaline (around 8.5) complete oxidation of ferrous ions occurs and  $\text{Fe}(\text{OH})_{3(\text{s})}/\text{FeOOH}_{(\text{s})}$  precipitates [69].

These results are in good agreement with the findings of other studies that ferrous ions are only oxidized to ferric ions if the pH is above 5 even though complete oxidation only occurs at pH of around 8-9 [25, 50, 57, 70]. At highly alkaline pH, undesired  $\text{Fe}(\text{OH})_4^-$  forms which is a weak coagulant and deteriorates EC performance [25, 57, 69]. It is therefore concluded that the optimum operating pH range of iron EC is 5-9 and operation at an initial pH of 8-9 is favorable to ensure complete oxidation of ferrous ions which are known to be highly soluble and considered as secondary pollutants as they increase the dissolved constituents in water.

### **2.3.6 *Electrode material***

Selecting the proper electrode material is critical since it determines the reactions that would take place and the type of metal coagulants generated. The selection criteria includes cost, availability, reliability and effectiveness of the metal electrode. As mentioned previously, Al and Fe electrodes are most widely used due to their proven reliability and availability. In most studies, it is generally proven

that Al electrodes enhance the efficiency of removing pollutants better than Fe electrodes [25]. Other than Al and Fe, a wide range of electrode materials were also tested; Hussin et al. compared the performance of zinc, copper, aluminum and iron electrodes for the removal of Pb(II) from aqueous solutions. The authors concluded that zinc electrodes were superior through achieving the highest removal of Pb(II) (97.5%) with minimum sludge generation and lowest energy consumption (0.325 kWh/m<sup>3</sup>) and operating cost (0.664\$/m<sup>3</sup>) within 30 minutes of operation [71].

In a recently published study, Kamaraj and Vasudevan investigated the effect of the anode material on the removal efficiency of radioactive materials such as strontium and cesium. The authors ran a set of experiments using aluminum, iron, zinc and magnesium anodes while keeping the galvanized iron cathode unchanged. Magnesium anode proved to be the most effective anodic material where it achieved a 97% removal of strontium and a 96.8% removal of cesium [72]. Genesan et al. achieved a 97.2 % removal of manganese from drinking water using an EC cell with magnesium anode and stainless steel cathode. The optimum operating conditions were 0.05 A/dm<sup>2</sup> and a pH of 7.

Govindan, Noel and Mohan studied the removal of nitrate ions from aqueous solutions through electro-denitrification process. Aluminum, iron and inert graphite electrodes were tested as anode and cathode materials and the effect on nitrate ion removal was observed. The authors reported that when aluminum and iron electrodes are used as anodes, the denitrification process took place through electrocoagulation as well as electro-reduction. In the case of electrocoagulation, the metal ions dissolving from the anode material leads to the removal of nitrate

ions. However, in case of electro-reduction, the nitrate ions are consumed in the ammonia production process. Therefore, when iron and aluminum ions were used, the nitrate removal was significantly higher than the ammonia production process. On the other hand, when non-dissolving graphite electrode was used, the ammonia production process was very close to the nitrate ion removal. The authors concluded that aluminum anode along with inert graphite cathode gave the best results by achieving a 92% reduction of nitrate ions [73].

Kumar et al. assessed the performance of iron, aluminum and titanium electrodes for the removal of arsenic from water. The results were more than 99% removal using iron electrodes, 37% removal using aluminum electrodes and 58% removal using titanium electrodes. Therefore iron electrodes were considered the most effective [74].

## **2.4 Challenges and recent advances in Electrocoagulation technology**

### **2.4.1 Challenges**

Although EC technology has been used for a few years, the available literature does not provide a systematic approach for EC reactor design and operation. EC is successfully used to treat water and wastewater at a laboratory scale, However, scaling up to meet industrial conditions is challenging; this is attributed to the fact that current research mainly focuses on removal of specific pollutants from wastewaters using batch experiments, “pollutant centered” approach. Very few authors take it to the next step and develop models for optimization and design of the reactor as a function of the operating conditions, “process centered” approach.



Such models will facilitate predicting the performance of EC reactors before actually designing them and will give researchers a better understanding of the design aspects, allowing EC technology to progress beyond the current state of impracticality.

As mentioned previously, EC integrates three different technologies; each of them is separately well established, but there is a lack of information on how these technologies could be practically integrated to come up with a reliable EC technology for industrial applications [35]. Therefore, it is crucial that researchers focus more on the study of the kinetics of the process and mathematical modelling in order to develop a deep understanding of the mechanism of EC technology.

Another major challenge that the technology is likely to encounter is that of high electricity consumption while treating the wastewater, as it directly affects the operating costs. Therefore, the success of this technology will depend on its ability to satisfy commercial criteria such as minimizing operational and maintenance costs and achieving profit on the investment made in the shortest time possible. The technology also faces strong competition from the existing well-established water treatment technologies such as adsorption, biotechnology and membrane technologies. Integration of EC technology with the existing technologies would improve its chances of success.

#### **2.4.2 *Recent advances***

Considerable efforts have been put in recent years to overcome the above-

mentioned challenges and improve the practicality of EC as an effective water treatment technology. This section highlights some of these efforts.

#### ***2.4.2.1 Integrating EC units with existing technologies***

As mentioned earlier, being able to integrate EC units with existing water treatment technologies is a major challenge. This was tackled by El-Naas et al. where they performed laboratory scale experiments to study the performance of EC cell integrated with a spouted bed bioreactor and an adsorption packed column to treat highly contaminated refinery wastewater. The best results were achieved when EC was used as a pretreatment step to reduce the contaminant loads prior to the following treatment steps. El- Naas et al.[75] took their novel design to the next step where they upgraded the bench scale units into a pilot scale plant with a 1.5 m<sup>3</sup>/h capacity. The EC unit was supplied by Powell water systems, Inc. which has over 25 years of experience in EC and wastewater treatment [75].

Modenes et al. [76] studied the treatment of tannery industrial effluent with an integrated photo-Fenton and electrocoagulation process. First, a full 3<sup>3</sup> factorial experimental design (FED) was applied to optimize the photo-Fenton process conditions. Then the effluent of the photo-Fenton process was treated using bench scale EC reactor with aluminum electrodes. The results showed that the proposed integrated process achieves better removal of organic and inorganic pollutants and generates less sludge compared to the conventional treatment method that combines filtration, chemical coagulation and sedimentation. Moreover, the integrated process proved to be an economically attractive alternative with minimum

environmental impact.

Manenti et al. [77] proposed a multistage process composed of electrocoagulation (using iron electrodes), photo-Fenton and activated sludge biological reactor for the treatment of real textile wastewater. The performance of the integrated system was assessed based on the dissolved organic carbon, chemical oxygen demand and biodegradability index. Using electrocoagulation as the first treatment step reduced the COD content by 36% then the effluent of EC was treated using photo-Fenton method which resulted in a 65% relative COD reduction and more than 70% biodegradability index. The final stage was the bioreactor which treated the effluent from the photo-Fenton process and was able to achieve a COD concentration within the allowable environmental legalization limit.

Bani-Melhem and Smith [78] investigated the effectiveness of integrating an electrocoagulation unit that uses aluminum electrodes with a submerged membrane bioreactor (SMBR) to treat grey water and compared the results with a standalone SMBR process. The results of the analysis showed that the integrated EC-SMBR process slightly enhances the removal percentage of turbidity, color and COD compared to the standalone SMBR and both processes were found to achieve 100% removal of suspended solids and fecal coliforms. Using EC as a pretreatment step before the SMBR not only enhanced the removal of pollutants but also reduced the membrane fouling by almost 13%.

Deghles & Kurt [79] used a hybrid electrocoagulation/ electro dialysis process to treat tannery effluent. The authors have optimized the electrocoagulation process by controlling various process parameters and then the effluent from

electrocoagulation process was further treated using electro dialysis. The electrocoagulation unit used five pairs of electrodes (iron or aluminum) in monopolar parallel mode. A bipolar membrane electro dialysis with platinized titanium electrode as anode and cathode in a pilot scale was then used to treat electrocoagulation effluent. The results showed that using hybrid electro dialysis/ electrocoagulation with iron electrodes achieved a removal efficiency of 87% COD, 100% NH<sub>3</sub>-N, 100% Cr and 100% color. On the other hand, using hybrid electro dialysis/ electrocoagulation with aluminum electrodes achieved a removal efficiency of 92% COD, 100% NH<sub>3</sub>-N, 100% Cr and 100% color.

#### ***2.4.2.2 Cell design and process enhancement***

Over the past years, efforts have been put to enhance the design of electrocoagulation reactors aiming to achieve higher efficiency and removal rates. This section highlights some of these efforts.

Nia'm & Othman [80] investigated the effectiveness of integrating magnetic fields with EC to enhance the removal and sedimentation of suspended solids from wastewater. An electrocoagulation unit with 15 monopolar iron plate electrodes arranged as baffles was used along with a permanent magnet "AlNiCo" with magnetic strength 0.16T placed under the reactor. The removal of suspended solids was optimized using response surface methodology "RSM" where the removal efficiency exceeded 92% at optimum conditions compared to 85.9% before applying the magnetic fields.

Hamdan & El-Naas [81] used an innovative electrocoagulation column to treat groundwater to be within drinking water limits. Iron was used for both electrodes

with a rod anode and a helical cathode inside a Plexiglas column operated in a continuous mode, with air mixing. At optimum conditions, 100% chromium removal was achieved at a minimum power consumption of 0.75 kWh/m<sup>3</sup>. In a similar study, Kobya et al. [82] compared the performance of two different electrocoagulation reactors in terms of the removal efficiency of arsenic from groundwater and operating costs. The first reactor used a cylindrical titanium cathode inside a Plexiglas cylinder, the cathode cylinder was filled with iron ball anode and another stainless steel rod was immersed in the iron balls to supply DC current when connected to an outer power supply. The second reactor consisted of two plate anodes and two plate cathodes both made of iron and connected in a monopolar parallel mode inside a Plexiglas cylinder. Air was supplied from the base of the two reactors to enhance mixing. The results revealed that at optimum conditions, the first reactor setup achieved 99.3% arsenic removal at an operating cost of 1.55\$/m<sup>3</sup> while the second setup achieved 96.9% arsenic removal at an operating cost of 0.1\$/m<sup>3</sup>.

El-Ashtoukhy et al. [83] studied the effectiveness of a novel electrocoagulation reactor to treat paper mill effluents. The reactor was made of a mechanically agitated cylindrical Plexiglas vessel with four baffles fixed at the inner wall of the vessel. The vessel was lined with lead sheet as the anode and a concentric stainless steel cylindrical screen as the cathode. The maximum COD and color removal achieved was 97% & 100% respectively while the minimum operating cost was 4 kWh/m<sup>3</sup>.

Abdelwahab et al. [61] examined the suitability of electrocoagulation to remove

phenol from real oil refinery effluent by using horizontally oriented aluminum electrodes inside a rectangular Plexiglas container. The horizontal plate cathode was placed at the bottom of the reactor with a single screen “mesh” or an array of closely spaced aluminum screens on top acting as the anode. The authors claim that using an array of aluminum screens as the anode increases its lifetime. At optimum experimental conditions, 94.5% phenol removal was achieved.

El-Ashtoukhy et al. [84] modified the cell design proposed by Abdelwahab et al. [61] to enhance the removal of phenolic compounds from oil refinery wastewater where they used a packed bed electrocoagulation reactor. The new reactor design consists of aluminum raschig rings randomly packed inside a perforated plastic container on top of a horizontal cathode. 100% removal of phenol was achieved at optimum conditions with lower operating cost which proves that the new packed bed reactor is more efficient than the previous reactor.

Chaudhary & Sahu [85] used a unique electrocoagulation reactor operated in a semi continuous mode to treat real sugar mill wastewater. The reactor composed of an aluminum cylinder operated as the cathode and the outer body of the reactor as well with three aluminum rods at the center of the cathode acting as the anode. For better mixing in the reactor, two baffle sheets fixed at the reactor inner wall were also used. In order to enhance the efficiency of COD removal, polyelectrolytes were used as coagulant aids where 80% COD removal was reached compared to 76% before using electrolytes. Although using polyelectrolytes enhances the performance of electrocoagulation, it leaves the process with the same disadvantages of chemical coagulation since it becomes an additive process.

Narayanan & Ganesan [86] proposed a stirred batch electrocoagulation reactor coupled with adsorption with granular activated carbon to treat synthetic wastewater containing hexavalent chromium . The electrocoagulation cell used an aluminum plate cathode and iron plate anode. Using the coupled electrocoagulation and adsorption process significantly enhanced chromium removal rates in shorter operating time and lower current density compared to conventional electrocoagulation process. The highest chromium removal efficiency at optimum conditions obtained using the coupled process was 97%.

Mountassir et al. [87] used a hybrid electrocoagulation and adsorption process using clay particles to treat textile wastewater. A basic electrocoagulation Pyrex reactor was used with single cathode and anode aluminum plates. The authors reported the same results as Narayanan & Ganesan [86] where clay particles increased the rate of pollutant removal in shorter operating time and lower current density compared to conventional electrocoagulation. Using clay particles improves bridging between particles and the flocs formed are larger, denser and easily settleable.

Can et al. [88] investigated the effect of combining electrocoagulation with chemical coagulation using polyaluminum chloride or alum as coagulant aids to treat textile wastewater. The reactor was made of Plexiglas with two aluminum anodes and two cathodes connected in a monopolar mode. The results revealed that using polyaluminum chloride salt along with electrocoagulation significantly increase COD removal to reach 80% compared to 23% with electrocoagulation only in just five minutes of operation. It is worth mentioning that the operating cost was

also decreased due to the lower electrical energy consumption in case of the combined process.

#### ***2.4.2.3 Scale up of EC units***

After several years of extensive research on EC technology, various commercial EC units became available in the market for industrial use over the past years, but still did not resolve the problems associated with the unreliable/short lifetime of the unit and high operating costs. F&T water solutions, a company that manufactures EC units with capacities ranging from 2 to 1000 GPM either fixed or portable units with the option of complete automation claims that their latest technology “Variable Electro Precipitator- VEP” overcomes the deficiencies of existing EC units. They use an enhanced flow path designed to achieve maximum retention time and instead of wet electrode connections, external connections are used to avoid overheating and failure of the reactor. The VEP EC units were tested for different industrial applications with different capacities, electrode connections and power where the results of these case studies prove them reliable [89].

Another example from industry is the Santa Clara Wastewater (SCWW), a private company located in Ventura County and California, they have been treating non-hazardous wastewater streams from a wide range of industries for over 40 years. Recently SCWW upgraded their facility to include EC units to replace traditional chemical precipitation technique. In the case of chemical precipitation, chemicals were added to physically remove pollutants (suspended and dissolved solids) through filtration, SCWW was spending 100,000 \$ on chemical additives on a



monthly basis for the removal of heavy metals only. After installing EC units, SCWW cut down the cost of chemicals per month to 10,000 \$ without compensating the quality of treated water. In addition to the remarkable reduction in operating cost, EC was found to decrease sludge generation by 90%. It is worth mentioning that EC unit require smaller carbon footprint since it's capable of removing various contaminants in a single reactor compared to traditional methods that would require a specific equipment to target the removal of each pollutant separately [90]

#### ***2.4.2.4 Cost analysis of Electrocoagulation***

The claimed high operating cost of electrocoagulation acts as a major disadvantage of the technology and renders it impractical for large industrial applications. The published literature lacks the optimization and assessment of electrocoagulation operating cost where only few papers analyzed the cost of electrocoagulation.

Bayramoglu et al. [91] performed an economic analysis for the treatment of textile wastewater by electrocoagulation. The total operating cost including energy consumption, electrode material, labor, sludge handling, maintenance and depreciation costs for a chemical plant treating 1000 m<sup>3</sup>/day of wastewater was calculated for different electrode materials ( Fe or Al) different connection modes, operating time, pH and current density. The results showed that monopolar parallel connection with iron electrodes at 30 A/m<sup>2</sup> current density, pH of 7 and 15 min operating time was the most cost effective option with 0.25 \$/m<sup>3</sup>. The authors also compared the cost of electrocoagulation and chemical coagulation for treating the same wastewater and found that chemical coagulation cost was 3.2 times higher

than electrocoagulation.

Khaled et al. [51] investigated the effect of various reactor design parameters on the efficiency and operating cost of electrocoagulation that targets the removal of cadmium from wastewater. The parameters investigated were distance between the electrodes, electrode connection mode, stirring speed, surface area to volume ratio (S/V) and initial temperature. Operating cost in this study was defined as the cost of electrodes (Aluminum), electrical energy and the cost of chemicals added for pH adjustment. The investigation revealed that 100% cadmium removal was achieved with very low power consumption and minimum operating cost of 0.116 TND (Tunisian National Dinar, equivalent to 0.06 USD) at the optimum conditions of 0.5 cm inter-electrode gap, 50 C initial temperature, 300 revolution/ min stirring speed, 13.5 S/V ratio and monopolar connection mode. The authors also reported the cost of chemical coagulation of the same process as 4.36 TND (2.1 USD) which shows that electrocoagulation is much more cost effective.

Rodriguez et al. [92] performed a techno-economic analysis for the treatment of metallurgic wastewater using electrocoagulation and chemical coagulation. Comparison of the results proved that for the same flowrate of wastewater (110 m<sup>3</sup>/y) the energy cost of electrocoagulation was 220 €/y (246.4 USD) while chemical coagulation was 106 €/y (118.7 USD) which is not surprising as electrocoagulation consumes electricity. On the other hand, the material cost for electrocoagulation was 440 €/y (492.8 USD) compared to 1100 €/y (1232 USD) which is also reasonable since chemical coagulation consumes large quantities of coagulant aids. From this comparison it could be seen that the total treatment cost

for electrocoagulation (660 €/y, 739 USD) is much less than chemical coagulation (1206 €/y, 1350.8 USD).

Kobyas & Demirbas [40] evaluated the effect of different parameters on the efficiency and operating cost of electrocoagulation to treat can manufacturing wastewater. At the optimum operating conditions of current density  $20\text{A/m}^2$ , operating time 40 min and monopolar parallel connection mode using aluminum electrodes, the operating cost was found to be  $0.366\text{ €/m}^3$  ( $0.41\text{ USD}$ ) of wastewater. Operating cost included the energy cost as well as the cost of electrode material.

Kobyas et al. [49] assessed the operating cost of treating real dye house wastewater with continuous flow electrocoagulation, operating cost was expressed as energy cost, electrode cost and chemical consumption cost. The authors found that at the optimum operating conditions of 80 min operating time,  $65\text{ A/m}^2$  current density and  $0.010\text{ L/min}$  flowrate, the cost using aluminum electrode was  $1.851\text{ \$/m}^3$  compared to  $1.562\text{ \$/m}^3$  using iron electrode. Lin et al. [93] designed and constructed a pilot-scale electrocoagulation unit to reclaim domestic grey water onsite for human non-contact use with a capacity of  $28\text{ m}^3/\text{day}$ . At optimum conditions, the total cost of the unit was  $0.27\text{ \$/m}^3$  which includes the capital and operational costs ( $0.08$  &  $0.19\text{ \$/m}^3$ ). The operating cost covers the energy cost, electrode cost, chemicals consumed and sludge treatment. The authors revealed that the unit cost and required area ( $8\text{m}^2$ ) are lower than the values reported in literature.

## **2.5 Overview of produced water composition**

Produced water is characterized by a very complex composition that varies depending on the reservoir type, the geographical location, reservoir depth, the geological formation and even the lifetime of a specific well. Therefore, samples of produced waters don't have identical composition. However, the typical constituents of produced water can be categorized into seven groups as described in the following subsections [4, 7, 94-98].

### **2.5.1 *Total dissolved solids (TDS)***

Dissolved solids or dissolved inorganic minerals are classified as anions and cations; the most abundant inorganic ions in produced water are sodium, chloride, calcium, magnesium, potassium, sulfate, bromide, and bicarbonate. Depending on the location and nature of the reservoir, other minerals including iodide, boron, lithium and strontium salts may exist as well [95]. Sodium and chloride ions are responsible for the extreme salinity of produced water, which exceeds seawater salinity in some cases. Typically, produced water salinity ranges from few parts per thousand to as much as 300 part per thousand, which is similar to concentrated brine. Sulfate ions usually exist in small concentrations in produced water compared to seawater. The presence of sulfate ions affects the solubility of other inorganic ions such as barium and calcium; an elevated concentration of sulfates may lead to scale formation due to the precipitation of calcium and barium sulfates [4]. Table 1 represents the typical range of the most common inorganic ions in oil and gas produced waters compared to seawater.

*Table 1: Inorganic constituents of oil & gas produced waters (PW) compared to seawater*

| Constituent   | Oil field PW (mg/L)<br>[99] | Gas field PW (mg/L)<br>[99] | Seawater (mg/L)<br>[10] |
|---------------|-----------------------------|-----------------------------|-------------------------|
| TDS/ salinity | -                           | 139,000- 360,000            | 35,000                  |
| Sodium        | 132-97,000                  | 37,500- 120,000             | 10,760                  |
| Chloride      | 80- 200,000                 | 81,500- 167,448             | 19,353                  |
| Sulfate       | 1,650                       | ND- 19                      | 2,712                   |
| Potassium     | 24- 4,300                   | 149- 3,8750                 | 387                     |
| Calcium       | 13- 25,800                  | 9,400- 51,300               | 416                     |
| Barium        | 1.3- 650                    | 9.65- 1,740                 | -                       |
| Magnesium     | 8- 6000                     | 1,300- 3,900                | 1,294                   |

**ND (not detected)**

### ***2.5.2 Total petroleum hydrocarbons***

Total petroleum hydrocarbons (TPHs) are defined as all organic compounds consisting of hydrogen and carbon atoms. TPH could be classified as shown in Fig. 1 according to the type of bond (single, double or triple) or the shape of the compound (cyclic or straight). The solubility of petroleum hydrocarbons in water

depends on their polarity and molecular weight. Polar compounds tend to dissolve in water and lower molecular weight compounds dissolve better than heavier compounds. In general, aromatic hydrocarbons tend to dissolve more in water compared to aliphatic compounds of the same molecular weight. Polyaromatic hydrocarbons PAHs (hydrocarbons with more than one benzene ring), phenols, organic acids and BTEX (benzene, toluene, ethylbenzene, xylene) are examples of soluble hydrocarbons. Other hydrocarbons which are not soluble in water are found in the form of dispersed oil such as high molecular weight PAHs and alkyl phenols [4, 95, 99]. Existing produced water treatment technologies can separate dispersed oils efficiently but not the dissolved hydrocarbons. Hence, dissolved hydrocarbons are discharged into the environment. TPHs can cause serious environmental concerns, as they contribute to the biological oxygen demand (BOD) which affects aquatic life besides being a toxic and persistent contaminant. In Qatar for instance, TPHs are the only regulated parameter in case of produced water discharge [4, 95, 99].

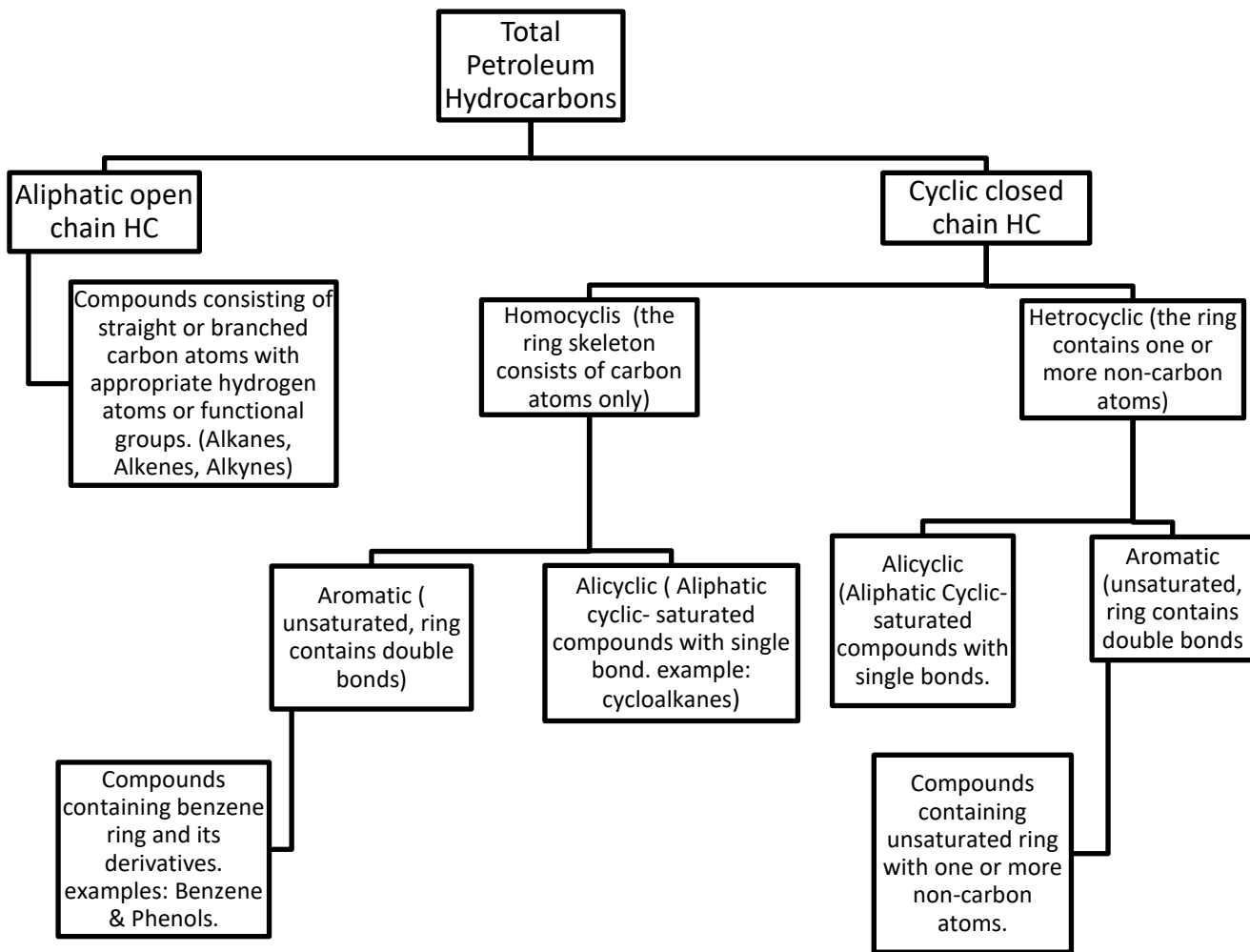


Figure 7: Classification of hydrocarbons [1]

### ***2.5.3 Dissolved & dispersed gasses***

Dissolved gases occur in produced water due to bacterial activities and chemical reactions. The most abundant dissolved gases in produced water are carbon dioxide, oxygen, and hydrogen sulfide [17, 95]. The solubility of gases in produced water is governed by Henry's law, which relates solubility to the temperature and partial pressure of the gas over the liquid (produced water). The pressure increases along the depth of the reservoir and so does the amount of dissolved gasses [95].

### ***2.5.4 Production chemicals***

Production chemicals are those compounds that are added to injection water for several purposes, such as scale & corrosion inhibition, wax deposition, gas dehydration, breaking emulsions, prevention of bacterial growth and for other means [17, 95]. Depending on the nature of the chemical additives, they could be more soluble in the oil phase than produced water and therefore will remain dissolved in oil and those more soluble in produced water are discharged with it. Due to the toxicity of some of the production chemicals and the environmental threats associated with their discharge, they should only be used if required and should not exceed the required optimum amount [4]. Table 2 illustrates the typical concentrations of various production chemicals in oil and gas produced waters.



*Table 2: Concentrations of typical production chemicals in oil and gas produced waters*

| Chemical                 | Concentration in oil field PW<br>[mg/L] [17] | Concentration in gas field<br>PW [mg/L] [17] |
|--------------------------|--|--|
| Corrosion inhibitor      | 2-10   | 2-10   |
| Demulsifier              | 1-2  | N.A  |
| Scale inhibitor          | 4-30   | N.A  |
| Polyelectrolyte          | 0-10   | N.A  |
| Methanol                 | N.A  | 1000-15000                                   |
| Di-ethylene glycol (DEG) | N.A  | 500-2000                                     |

N.A (Not Applicable)

### **2.5.5 Produced solids**

Produced water is extracted along with various types of production solids represented as clay, sand, silt, scale and corrosion products, wax and suspended solids. The removal of these solids is crucial to prevent clogging of pipes, the formation of oily sludge and other operational problems [4, 7, 17].

### **2.5.6 Heavy metals**

Produced water may contain a wide range of heavy metals depending on the source (oil/gas fields), geological formation, the age of the well, geographic location and other parameters. Typically, the following heavy metals are usually found in produced waters: cadmium, chromium, mercury, lead, arsenic, iron, zinc, manganese, silver, and copper [7, 95, 99]. The presence of heavy metals in produced water and discharging of such metals into the environment can have detrimental effects on aquatic life. Table 3 summarizes the typical concentration of heavy metals in oil and gas produced waters compared to seawater.

Table 3: Concentration of heavy metals in oil and gas produced waters, adapted from [99]

| Heavy metal | Concentration in oil field PW (mg/L) | Concentration in gas field PW (mg/L) | Concentration in seawater (mg/L) |
|-------------|--------------------------------------|--------------------------------------|----------------------------------|
| Arsenic     | 0.005- 0.3                           | 0.005-151                            | 1-3                              |
| Lead        | 0.002- 8.8                           | 0.2- 10.2                            | 0.001-0.1                        |
| Mercury     | 0.001-0.002                          | -                                    | 0.00007-0.006                    |
| Cadmium     | 0.005-0.2                            | 0.02-1.21                            | 3-34                             |
| Chromium    | 0.02-1.1                             | 0.03                                 | 0.1-0.55                         |
| Iron        | 0.1-100                              | 39-860                               | 0.008-2                          |
| Zinc        | 0.01-35                              | 0.02-5                               | 0.006-0.12                       |
| Silver      | 0.001-0.15                           | 0.047-7                              | -                                |
| Copper      | 0.002-1.5                            | 0.02-5                               | 0.03-0.35                        |

### 2.5.7 Naturally occurring radioactive materials (NORM)

Naturally occurring radioactive materials (NORM) are usually present in produced water as a result of the decay of certain rocks and clays in the hydrocarbon reservoir which contains uranium- 238 and thorium-232. The decay of these two radioactive elements results in the presence of radium-236 & radium-238 in produced water which are the most abundant types of NORM nucleoids. The rate of radioactive decay of these elements is measured in picocuries/L (pCi/L); one pCi is equivalent to 2.22 disintegrations per minute (dpm). Table 4 lists the typical activity of Ra-226 and Ra-228 in produced water compared to seawater [4].

*Table 4:* Typical activities of radium isotopes in produced water and sea water [4]

| Radionuclide | Produced water | Seawater   |
|--------------|----------------|------------|
| Ra-226       | 0.054 – 32,400 | 0.027-0.04 |
| Ra-228       | 8.1 - 4860     | 0.005-0.03 |

## **2.6 Environmental regulations for produced water discharge**

The overview of produced water composition discussed in the previous section illustrates that produced water discharge must be strictly regulated, as it is generated in huge quantities in addition to being heavily polluted. In countries/ regions with water scarcity issues, the problem is even more critical due to the limited available water resources [6]. For these countries, discharging of PW without proper treatment will not only pollute the available water resources, but will also waste the large amounts of PW that could be reused for irrigation, landscaping, and other beneficial uses after proper treatment. The most common approach used for PW treatment prior to discharge is oil/water separation, which is an efficient technique for removing suspended oils as mentioned previously. However, the dissolved contaminants including oils, heavy metals and the production chemicals when discharged along with PW into surface water, pose toxic effect to aquatic life. These contaminants can also contaminate soil and underground water [17].

Although it is agreed worldwide that PW discharge can cause serious environmental concerns, the standards/ regulations of PW discharge vary from one country to another. On the international level, the United States Environmental Protection Agency (USEPA) is the most recognized regulatory institution that regulates and enforces laws for produced water extraction and discharge. On the national level, each country should have an institution that regulates and enforces laws related to PW discharge for the country and must be followed by all operating companies [95]. According to EPA, the pollutants are divided into three major groups: “conventional pollutants (five-day biochemical oxygen demand, total suspended solids, pH, fecal coliform, and oil and grease), toxic or priority pollutants

(including metals and man-made organic compounds), and nonconventional (including ammonia, nitrogen, phosphorus, chemical oxygen demand, and whole effluent toxicity)” [100]. EPA has developed effluent limitation guidelines (ELGs) tailored to each industry and represent the maximum pollutant reductions based on the best available technology. For oil and gas industry, ELGs are available for onshore, offshore, and coastal operations as well. For PW generated onshore, the maximum allowable oil & grease content is 35 mg/L prior to discharge; moreover, the quality of PW must be reasonably good to be used for irrigation or for livestock. In cases where the PW generated from onshore facilities will not be used for livestock or agriculture, then PW discharge from such facilities is prohibited by EPA and a “zero-discharge” is implemented. For PW generated from offshore, the EPA has set a maximum daily oil & grease limit of 42 mg/L and a monthly average limit of 29 mg/L [100]. For PW reinjection in reservoirs or aquifer, EPA limits the oil & grease content to 30 mg/L. It could be noticed that the only regulated parameter when it comes to PW reinjection or discharge is oil & grease, where it is considered as a representative of other pollutants. When oil and grease are controlled, other pollutants will also be controlled [101]. On the regional level, several conventions/ treaties were held with the aim of limiting the discharge of pollutants into the environment. The major conventions such as the Oslo and Paris Commission for the North-East Atlantic (OSPAR), the Barcelona Convention for Mediterranean countries, the Kuwait Convention and the Helsinki Convention (HELCOM Convention) for the Baltic are listed in Table 5 [104].

*Table 5: Maximum allowable O&G limit for PW discharge according to regional convention*

| Legal Basis   | Oil and grease limit for PW discharge                      |
|---|--|
| OSPAR Convention(North Sea countries)<br>[102]                        | 30 (mg/L)  |
| Baltic Sea Convention and HELCOM<br>standards [103]                   | 15 (mg/L)] max; 40 mg/l if BAT cannot<br>achieve 15 (mg/L) |
| KUWAIT Convention and Protocols (Red<br>Sea region) [104]             | 40 (mg/l), 100 (mg/L) max                                  |
| Barcelona Convention and Protocols<br>(Mediterranean countries) [104] | 40 (mg/l), 100 (mg/L) max                                  |

## **2.7 Applications of Electrocoagulation for produced water treatment**

In a recently published review paper, Moussa et al. presented a detailed review of the applications of EC for different types of water and wastewater. The authors cover six different categories namely; Water containing heavy metals, Tannery and textile industry wastewater, food industry wastewater, paper industry wastewater, refinery wastewater, and produced water [2]. For this thesis, the focus will be on the recent applications of EC for produced water treatment only which is summarized in Table 6.

Table 6: Applications of EC for produced water treatment

| Technology                | Anode material                         | Scale of operation     | Targeted contaminants  | Maximum removal efficiency   | Energy use / treatment cost | Current density   | Treatment time | Reference |
|---------------------------|--|------------------------|--|--|-----------------------------|---|----------------|-----------|
| <b>Electrocoagulation</b> | Fe & Al (Polarity reversed every 90 S) | Lab scale (continuous) | Magnesium<br>Calcium<br>Barium<br>Strontium<br>Boron<br>TOC<br>Turbidity | 90% (Calcium)<br>70% (Magnesium)<br>61.1% (Strontium)<br>74.2% (Barium)<br>74% (Boron)<br>64% (TOC)<br>More than 95% (Turbidity) | -                           | -   | 35 min         | [105]     |
|                           | Aluminum + biochar                     | Lab scale              | Turbidity<br>TSS<br>COD  | 99% TSS & Turbidity<br>5-14% COD   | 0.15 kWh/kg TSS             | Positive current (11.3 A/m <sup>2</sup> )<br>Negative current (6.7 A/m <sup>2</sup> ) | 30 min         | [106]     |
|                           | Fe & Al                                | Lab scale (Continuous) | COD  | 82.9% COD-Fe<br>74.9 % COD-Al  | -                           | 20 mA/cm <sup>2</sup>   | 45 min         | [107]     |
|                           | Iron                                   | Pilot scale            | Hardness<br>COD<br>Turbidity   | 85.81% (Hardness)<br>66.64% (COD)<br>93.8% (Turbidity)   | -                           | 5.90 mA/cm <sup>2</sup>   | 31 min         | [108]     |
|                           | Aluminum                               | Batch                  | Oil & Grease<br>Turbidity  | 90%  | 0.12 kWh/kg oil (approx.)   | 6.8 mA/cm <sup>2</sup>  | 90 min         | [109]     |
|                           | Aluminum                               | Batch                  | Boron  | 98%  | -                           | -   | 90 min         | [110]     |



## Chapter 3

### 3.1 Experimental setup

A novel EC cell has been designed and tested in this work. The new cell design, shown in Figure 8, was fabricated at the engineering workshop at Qatar University, using available materials and resources. The setup consists of three 1.8 L cylindrical Plexiglas vessels for the feed tank, reactor cell and settling tank. The electrodes were made of iron and aluminum (commercial grade) with different geometries and same surface area (83.7 cm<sup>2</sup>). For each metal electrode, three different configurations were used for the sake of comparison: plate electrodes, cylindrical electrodes and perforated hollow cylindrical electrodes. An air compressor was used to supply air bubbles at a flowrate of 15 standard cubic feet per hour (SCFH) for mixing and/ or cleaning the electrodes. In the case of perforated hollow cylindrical electrodes, air was injected through the top of the electrode and allowed to diffuse from the perforations upward along the electrode surface, where it acts as a passivation prevention mechanism. A Rigol DC power supply was externally connected to the electrodes with adjustable current input. The system was tested and optimized in a batch mode of operation (Figure 9) and then operated continuously at the optimum conditions.

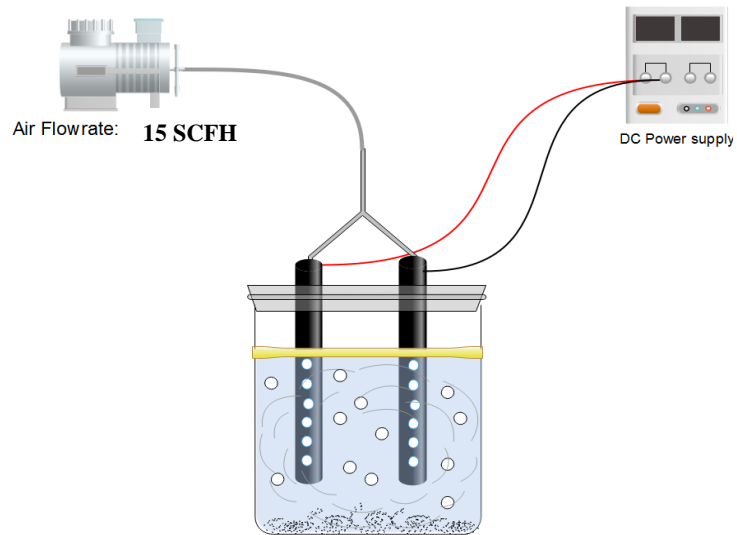


*Figure 8: Illustration of batch EC setup*

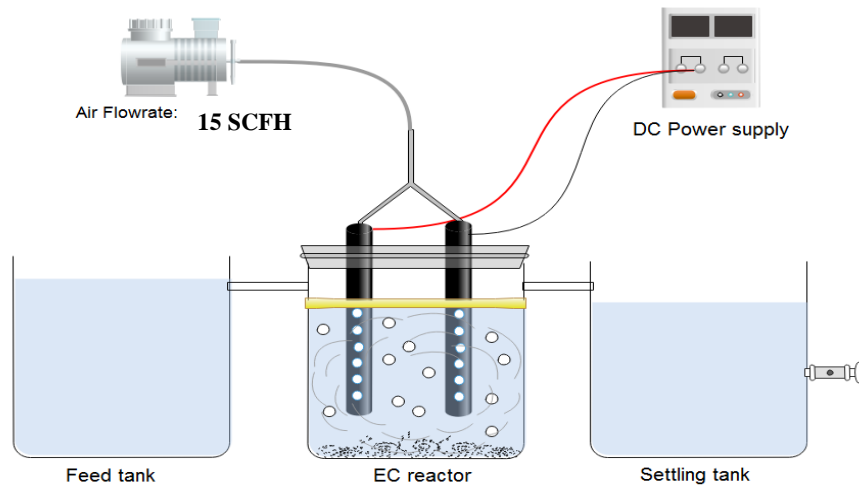


*Figure 9: Illustration of continuous setup*

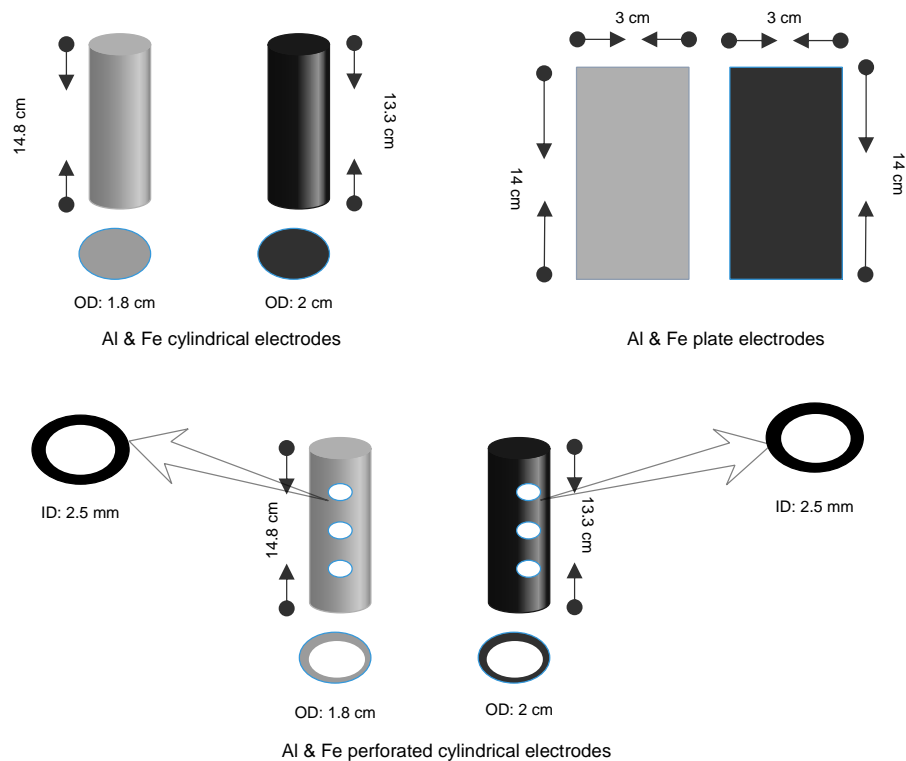


Figure 10: Electrode configurations and dimensions

## 3.2 Materials and methods

### 3.2.1 Synthetic produced water preparation

The initial plan was to obtain real produced water from Qatar's natural gas fields for the experiments; however, it was not possible to obtain real produced water due to certain restriction set by the gas fields.. Therefore, synthetic produced water samples were prepared and used for experimentation.. Based on the literature review (Chapter 2)it could be seen that produced water has similar constituents to those of seawater with different concentrations; however, produced water is usually more saline and more contaminated

than seawater. Therefore, using seawater was preferred over synthesizing produced water from deionized water and chemical additives, as the later method usually excludes trace elements that exist in both seawater and real produced water. The collected seawater had a conductivity ranging between 40-45 mS/cm. The seawater was evaporated to increase its salinity and conductivity to be within the desired value; a commercial crude oil with a density of 900 kg/m<sup>3</sup> was then added slowly and mixed using a high speed homogenizer for 15 minutes. The characteristics of the synthetic produced water used for this work is shown in Table 7.

*Table 7: Characteristics of synthetic produced water*

| <b>Parameter</b>    | <b>Value</b> |
|---------------------|--------------|
| <b>pH</b>           | 7.5          |
| <b>Conductivity</b> | 120 ms/cm    |
| <b>TDS</b>          | 97 g/L       |
| <b>O&amp;G</b>      | 360 ppm      |
| <b>TOC</b>          | 350 ppm      |
| <b>TPH</b>          | 2300 ppm     |

### 3.2.2 *Experimental analysis*

1. **Oil and grease analysis:** standard USA EPA method (1664 A) was used for oil and grease analysis.
2. **Total Petroleum Hydrocarbons:** standard USA EPA non-halogenated organics using gas chromatography/ flame ionized detector (GC/FID) (8015 C modified) was used for TPH analysis.
3. **Chemical Oxygen Demand (COD):** HACH, digital reactor block (DRB-200) and benchtop spectrophotometer (DR 3900™) were used for COD analysis.
4. **Total Organic Carbon (TOC):** Samples were analyzed for TOC using “TOC-L-CSH” device supplied by Shimadzu Corporation.
5. **pH:** YSI, EcoSense (pH100) pH meter was used for pH measurements.
6. **Conductivity and Total Dissolved Solids:** YSI, EcoSense (EC-300) conductivity meter was used for conductivity and TDS measurements.
7. **Sludge characterization:** Rigaku, MiniFlexII desktop X-ray diffractor device was used for sludge characterization.

### 3.2.3 *Experimental procedures*

In order to test the performance of the newly proposed cell design, several experiments were performed based on the following steps:

- 1- **Select electrode material:** Basic plate aluminum and iron electrodes were used to perform batch EC experiments at fixed conditions of 15 mA/cm<sup>2</sup> current density, 15 standard cubic feet per hour (SCFH) air flowrate and a duration of 30 min. The treated water was then analyzed using chemical oxygen demand (COD), total

organic carbon (TOC), total petroleum hydrocarbons (TPH) and Oil & Grease (O&G) analysis.

- 2- **Select electrode geometry:** For the selected electrode material, the cylindrical and perforated hollow cylindrical electrodes were tested with different combinations for EC experiments at the same conditions mentioned above. The treated samples were analyzed for the same parameters as before and the optimum electrode geometry was selected.
- 3- **Optimize the performance of selected electrode setup:** In order to optimize the system performance, a multivariate statistical technique known as response surface methodology (RSM) was used to predict the optimum operating conditions after performing a set of experiments based on the selected experimental design and observing the response.
- 4- **Test the optimum design for continuous mode of operation:** After selecting the optimum design and operating conditions, the system was run in a continuous mode of operation. This step is essential to examine the effect of bubbling air from perforated cathode on the system performance and minimizing passivation on the long run. A schematic diagram of the experimental sequence is shown in Figure 11.

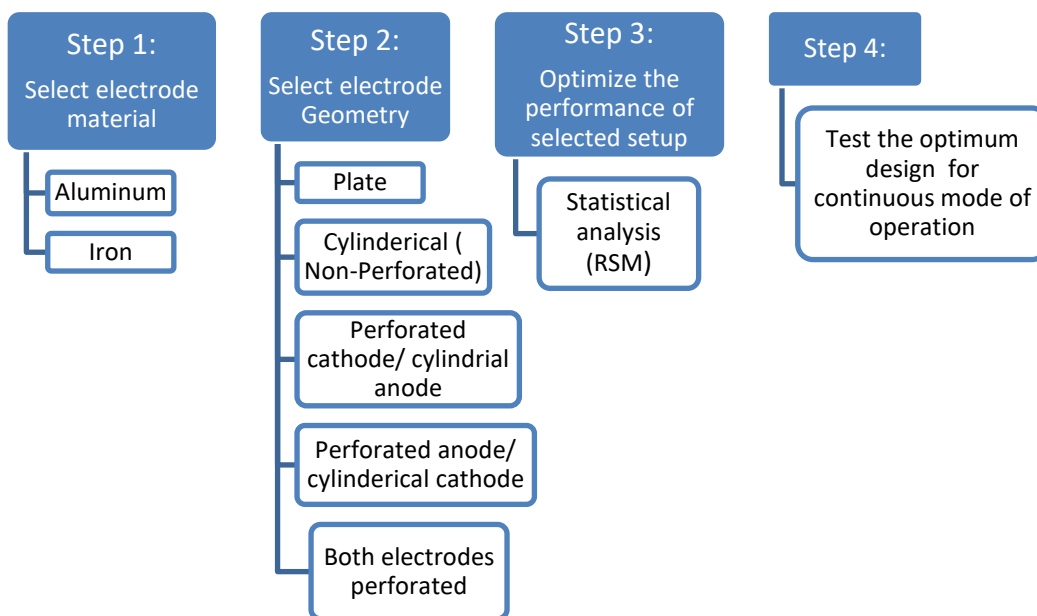


Figure 11: A schematic diagram of the experimental steps

## Chapter 4: Results & Discussions

### 4.1 Selection of electrode material

The treated water samples using both aluminum and iron plate electrodes were analyzed for COD, TOC, TPH and O&G. The results of each analysis are discussed below:

#### 4.1.1 COD results

Table 8 summarizes the COD results using the high range Hach COD vials (LCK-514) which covers a COD range of 150- 2000 mg/L COD. The samples were diluted 10 times.

*Table 8: COD results using high range vials*

| Sample            | Dilution | COD reading<br>(mg/L) | Actual COD concentration<br>(mg/L) |
|-------------------|----------|-----------------------|------------------------------------|
| PW<br>(Untreated) | 10 times | 170                   | 1700                               |
| AL (treated)      | 10 times | 101<br>(below range)  | 1010                               |
| FE (treated)      | 10 times | 117<br>(below range)  | 1170                               |

Using high range vials with 10 times dilution, the COD concentrations were below the detectible limit in case of aluminum and iron treated PW. Therefore, a low range Hach COD vials (LCK 314) which covers a COD range of 15-150 mg/L were used instead with 10 times dilution. Table 9 summarizes the results.



Table 9: COD results using low range vials

| Sample         | Dilution | COD reading<br>(mg/L) | Actual COD concentration<br>(mg/L) |
|----------------|----------|-----------------------|------------------------------------|
| PW (Untreated) | 10 times | 96                    | 960                                |
| AL (treated)   | 10 times | 68                    | 680                                |
| FE (treated)   | 10 times | 68                    | 680                                |

It could be seen that COD results were not reproducible using the high and low range vials. It was expected that COD concentration in PW would be above the detectable limit of low range vials as shown from the high range vials' results. However, the COD reading was only 96 with low range vials compared to 170 with high range vials. Moreover, low range vials shows identical COD readings for both aluminum and iron treated water samples (68 mg/L) which again contradicts the results from high range vials (101 mg/L for aluminum & 117 mg/L for iron). Knowing that the water samples are highly saline, it is possible that chloride interference is significant. Both high range and low range vials could tolerate a chloride concentration of 1500 mg/L maximum. To check the concentration of chloride ions in water samples, Hach chloride cuvettes (LCK-311) which cover a range of 70- 1000 mg/L chloride ions were used. Table 10 summarizes the results after 20 times dilution.

Table 10: Chloride cuvette test results

| Sample         | Dilution | Cl <sup>-</sup> reading<br>(mg/L) | Actual Cl <sup>-</sup> concentration<br>(mg/L) |
|----------------|----------|-----------------------------------|--|
| PW (Untreated) | 20 times | 2,522<br>( above limit)           | 50,440   |
| AL (treated)   | 20 times | 2,255<br>( above limit)           | 45,100   |
| FE (treated)   | 20 times | 2,223<br>( above limit)           | 44,460   |

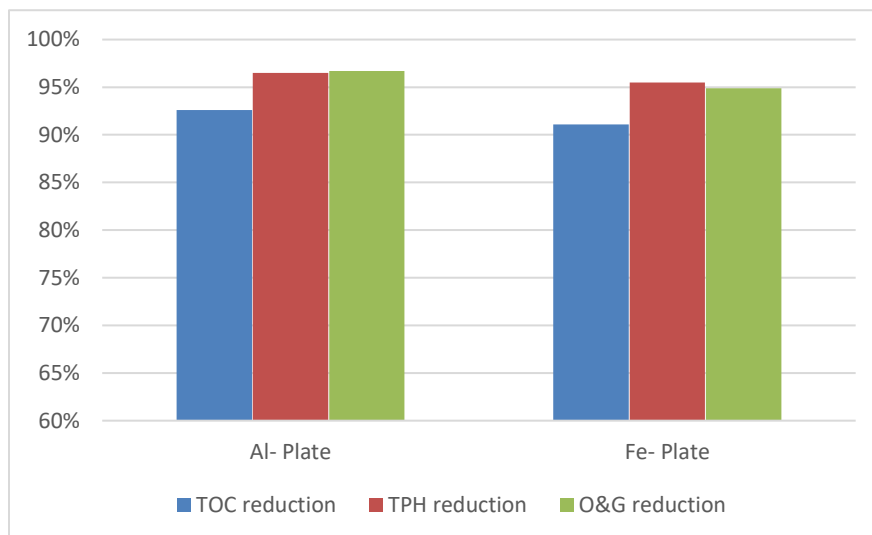
Although all samples were diluted 20 times, the chloride ion concentrations were more than double the maximum detectable limit (1000 mg/L Cl<sup>-</sup>). This explains the contradicting results when high and low range COD vials were used with only 10 times dilution. From the chloride cuvette test results, in order to achieve an acceptable chloride concentration, at least 40 times of dilution is required. Diluting the samples 40 times, however, will also reduce the COD concentration that it falls below the detectable limit of both vials. Therefore, COD analysis were excluded from the screening process as the results were unreliable.

#### 4.1.2 TOC, O&G and TPH results

Water samples were also analyzed using TOC analyzer, O&G and TPH and the results are summarized in Table 11. All samples were allowed to settle down completely before the analysis and only the clear layer was analyzed.

*Table 11:* Performance comparison of aluminum and iron electrodes

| Sample           | TOC removal | TPH removal | O&G removal |
|------------------|-------------|-------------|-------------|
| Al treated water | 92.6 %      | 96.5 %      | 96.7 %      |
| Fe treated water | 91.1 %      | 95.5 %      | 94.9 %      |



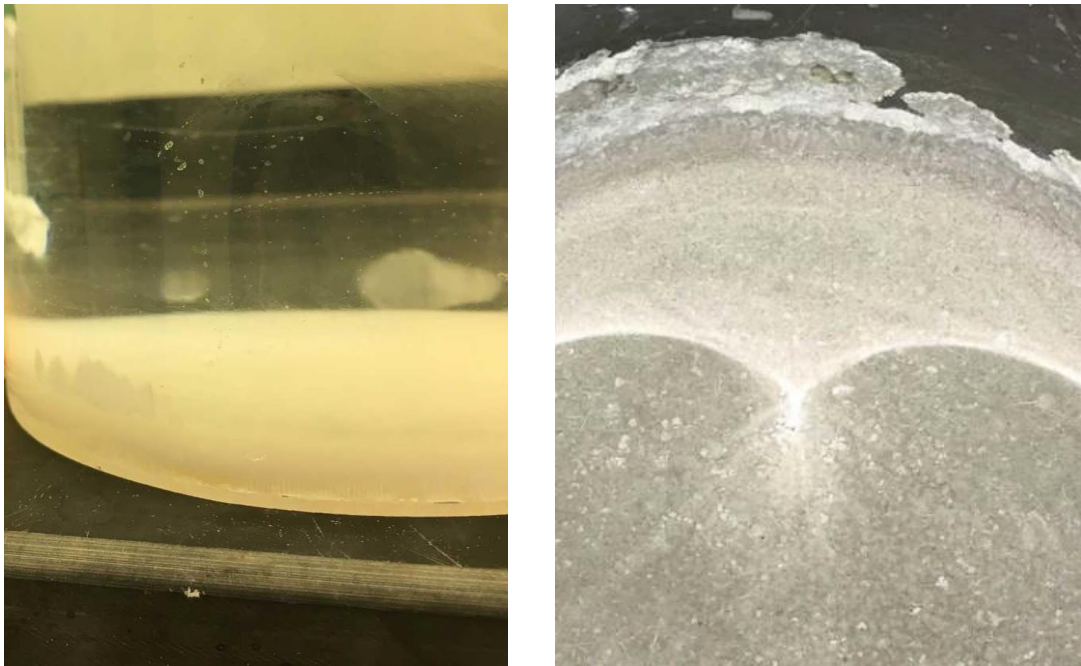
*Figure 12: Performance of aluminum and iron plate electrodes*

Table 11 and Figure 12 illustrate that aluminum electrodes are more effective compared to iron electrodes. Although both electrodes achieved good removal of all parameters and the results are quite close, aluminum electrodes are preferred to iron electrodes as iron electrodes turns the water color into a yellowish color due to the formation of iron rust and the color doesn't change even after the sample is allowed to settle down. Moreover, aluminum electrodes were easier to clean using sand filter compared to iron electrodes which corrode heavily after each run. Therefore, aluminum was selected as the optimum electrode material.

#### **4.1.3 Sludge characterization**

The sludge of both aluminum and iron (Figure 13 & 14) treated water samples was dried in oven at 110 °C for 8 hours and then analyzed using XRD. In case of aluminum

electrodes, the sludge had a white/ grey color which is expected due to the formation of  $\text{Al}(\text{OH})_3$ , the most stable form of aluminum at the pH of 7.5. XRD of aluminum sludge (Figure 15) proved that gibbsite (aluminum hydroxide-  $\text{Al}(\text{OH})_3$ ) was the predominant mineral besides calcite (calcium carbonate-  $\text{CaCO}_3$ ) and sodium carbonate ( $\text{Na}_2\text{CO}_3$ ).



*Figure 13:* Aluminum sludge



*Figure 14:* Iron sludge

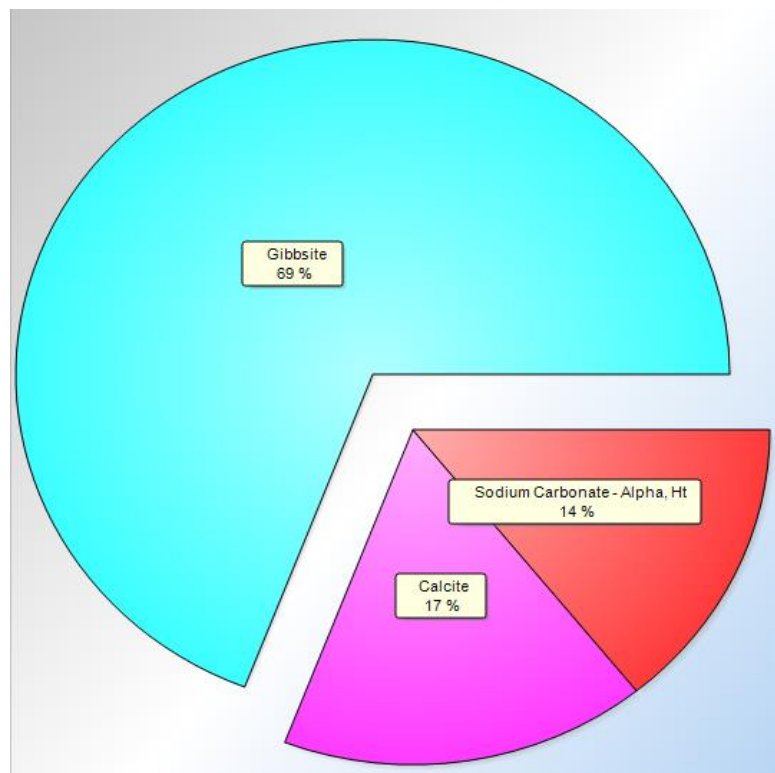
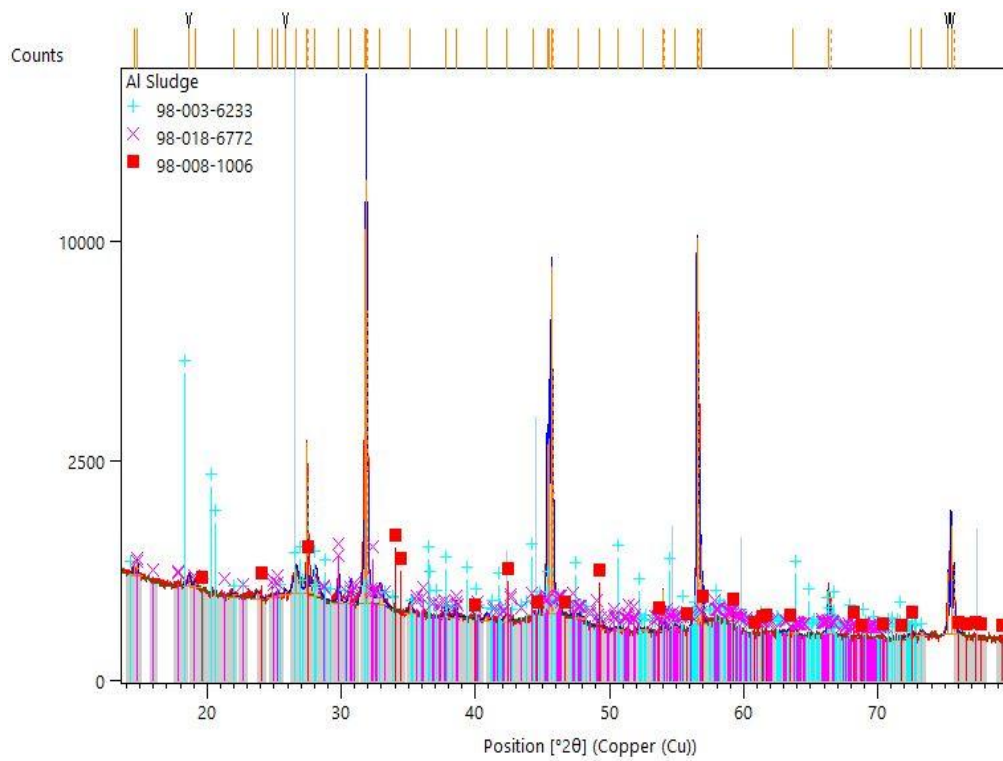
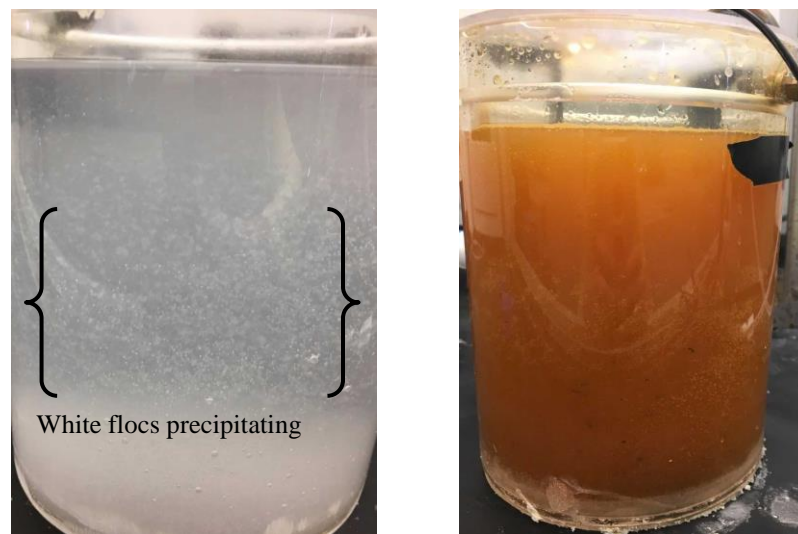


Figure 15: Al Sludge characterization using XRD

It was also noticed that the floc sizes in case of aluminum electrodes are bigger and could be seen by naked eyes which lead to faster settling and better removal of pollutants (Figure 16)

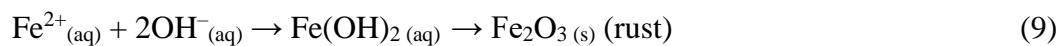


*Figure 16:* Comparison between aluminum and iron floc size

Iron sludge on the other hand had a reddish brown color due to the formation of iron rust. The XRD of iron sludge (Figure 17) showed that hematite ( $\text{Fe}_2\text{O}_3$ ) is the predominant mineral along with magnetite ( $\text{Fe}_3\text{O}_4$  or  $\text{FeO}\cdot\text{Fe}_2\text{O}_3$ ), iron carbonate ( $\text{FeCO}_3$ ) and sodium carbonate ( $\text{Na}_2\text{CO}_3$ ). Although the formation of ferric and ferrous hydroxides ( $\text{Fe}(\text{OH})_2$  /  $\text{Fe}(\text{OH})_3$ ) was predicted, none of them was found in iron sludge.



A possible explanation would be that the system was operated with continuous supply of air at an initial pH of 7.5. Under these highly oxidizing conditions, rust (Fe<sub>2</sub>O<sub>3</sub>) is the most stable form of iron and it forms according to the following equation.



From the literature review, it was also found that to ensure complete oxidation of ferrous ions to ferric ions and the formation of ferric hydroxide, operating at pH of 8-9 is desired. At lower pH (6.5-7.5), which is the case in the tested system, the rate of ferrous ions oxidation and hydrolysis is slow. This explains the change of treated water color (Figure 16) in case of iron electrodes and the lower removal efficiencies compared to aluminum electrodes.

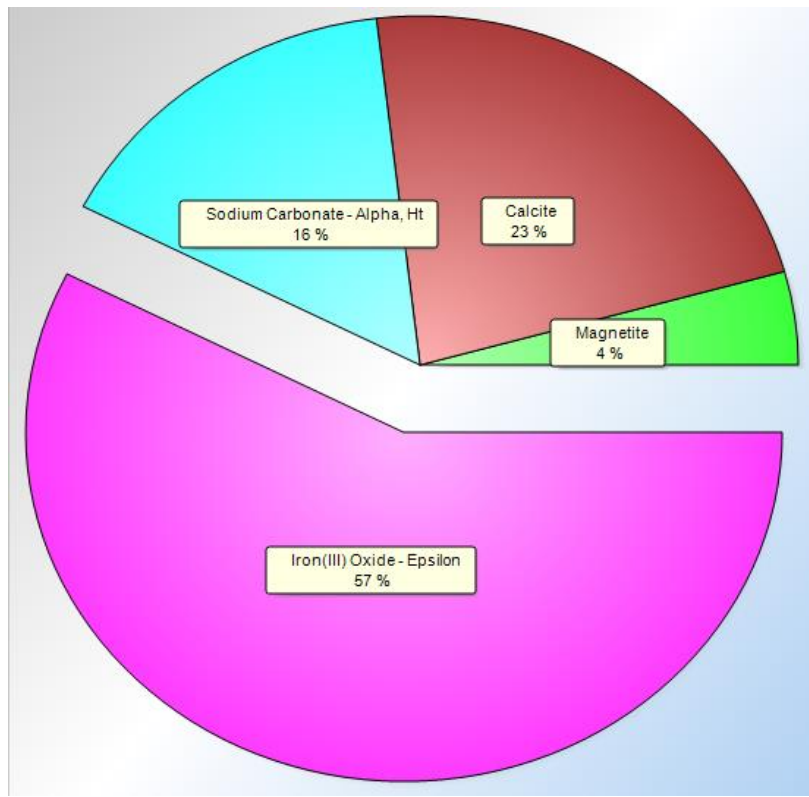
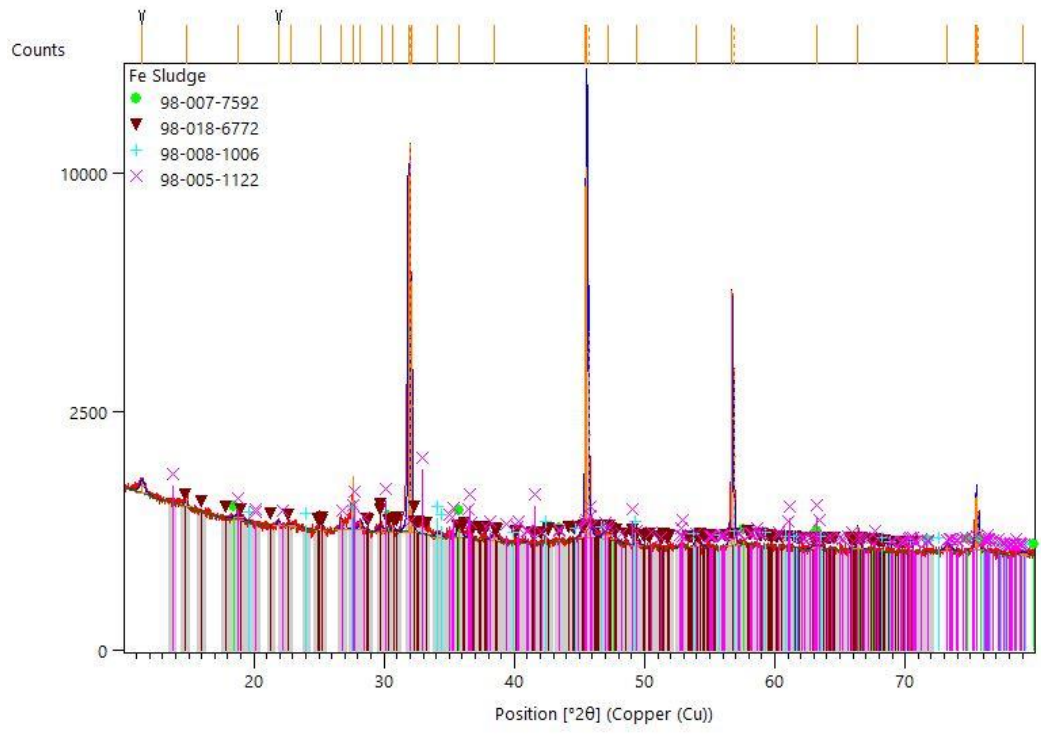


Figure 17: FE Sludge characterization using XRD

## 4.2 Selecting electrode geometry

### 4.2.1 TOC, O&G and TPH results

After selecting aluminum as the optimum electrode material, the next step was to decide on the electrode geometry. Four experiments were conducted using non-perforated cylindrical electrodes (anode and cathode- Al-NPR), perforated cylindrical electrodes (anode and cathode- Al-PR), perforated cylindrical anode with non-perforated cylindrical cathode (Al-PR-A) and non-perforated cylindrical anode with a perforated cylindrical cathode (Al-PR-C). All experiments were run at the same conditions as before for the sake of comparing the performance of different geometries. The treated water samples were also analyzed for TOC, O&G and TPH and the results are summarized in Table 12.

*Table 12: Performance comparison of different electrode geometries*

| Sample   | TOC reduction | TPH reduction | O&G reduction |
|----------|---------------|---------------|---------------|
| Al-Plate | 92.6 %        | 96.3 %        | 94.9 %        |
| Al-PR-A  | 95.7 %        | 96.7 %        | 96.3 %        |
| Al-NPR   | 97.1 %        | 97%           | 96.8%         |
| Al-PR    | 97.7%         | 97.3%         | 97.2%         |
| Al-PR-C  | 98.3 %        | 99 %          | 98.1 %        |

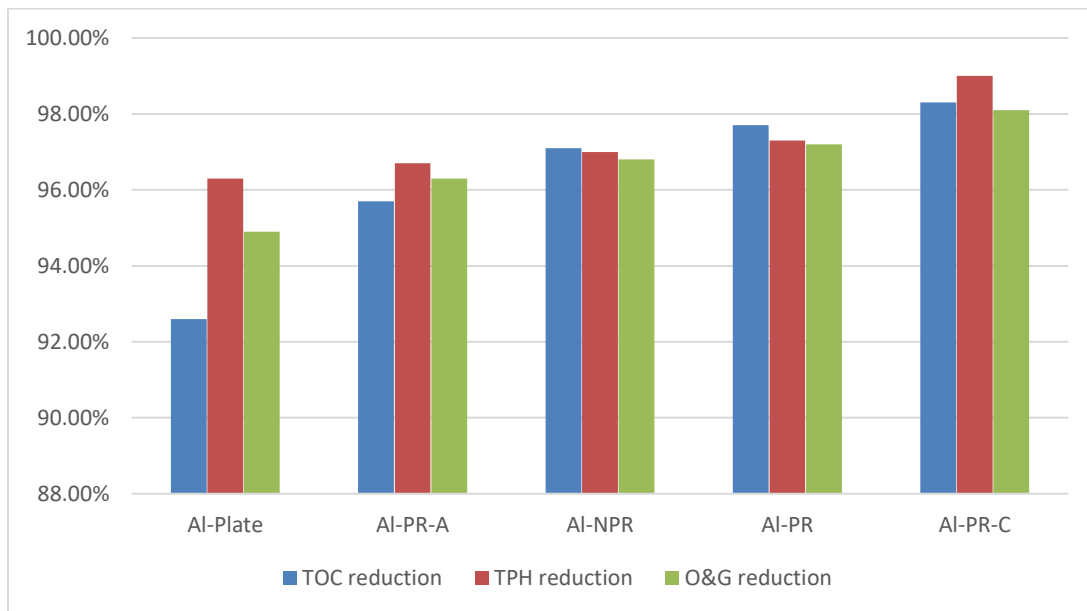


Figure 18: TOC, TPH and O&G reduction with five different aluminum electrode geometries

Table 12 and Figure 18 show that out of the five electrode geometries, aluminum plate electrodes gave the least removal followed by perforated anode with a non-perforated cathode. When only the anode was perforated, the intensity of air flowing from the anode perforations was very high that it formed a film of air bubbles on the anode surface, thus, partially isolating the anode surface from the solution. Moreover, the cathode was not perforated and passivation was not eliminated by any means. When both non-perforated cylindrical anode and cathode were used, with air supplied within the solution as a mixing tool only, the performance was slightly better as cylindrical electrode geometry is expected

to result in better metal ion distribution compared to rectangular plate geometry and the anode surface was now fully exposed to the solution.

In case of perforated cylindrical anode and cathode, the performance was even better as the air flowing from cathode perforations is expected to minimize the effect of passivation. In addition to that, pumping air from both electrodes provides more efficient mixing and decreases the intensity of air bubbles flowing from anode perforations. Finally, using a non-perforated anode along with a perforated cylindrical cathode gave the best results, since allowing the air to flow only from the cathode gave a stronger air flow compared to dividing the same air flowrate on two electrodes. Having a stronger air flow is expected to have better cleaning effect on the cathode surface to prevent passivation.

It is worth mentioning here that all electrode geometries performed well and the removal efficiencies were quite close since all of them had the same surface area. The effect of passivation on the removal efficiency will not be significant within 30 minutes of operation. Therefore, the best way to observe the effect of passivation on the system performance is by looking at the potential difference between the electrodes and power consumption.

#### ***4.2.2 Power consumption and potential difference between the electrodes***

The initial and final potential difference was recorded for the five electrode geometries and summarized in Table 13. All experiments were run for 30 minutes at the same conditions of 15 mA/cm<sup>2</sup> and 15 SCFH air flowrate. The corresponding power consumption was calculated at the average potential difference using the following equation:

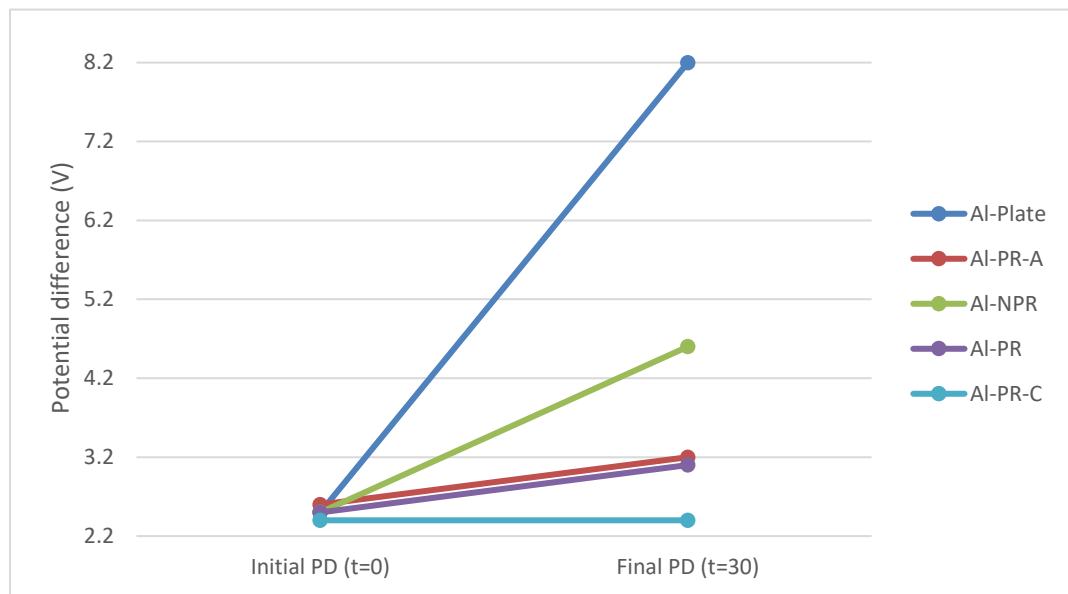
$$P \text{ (Watt)} = I \text{ (Amp)} \times V_{avg} \text{ (Volt)} \quad (10)$$

*Table 13* : Power consumption and potential difference for different electrode geometries at a fixed current of 1.3 A.

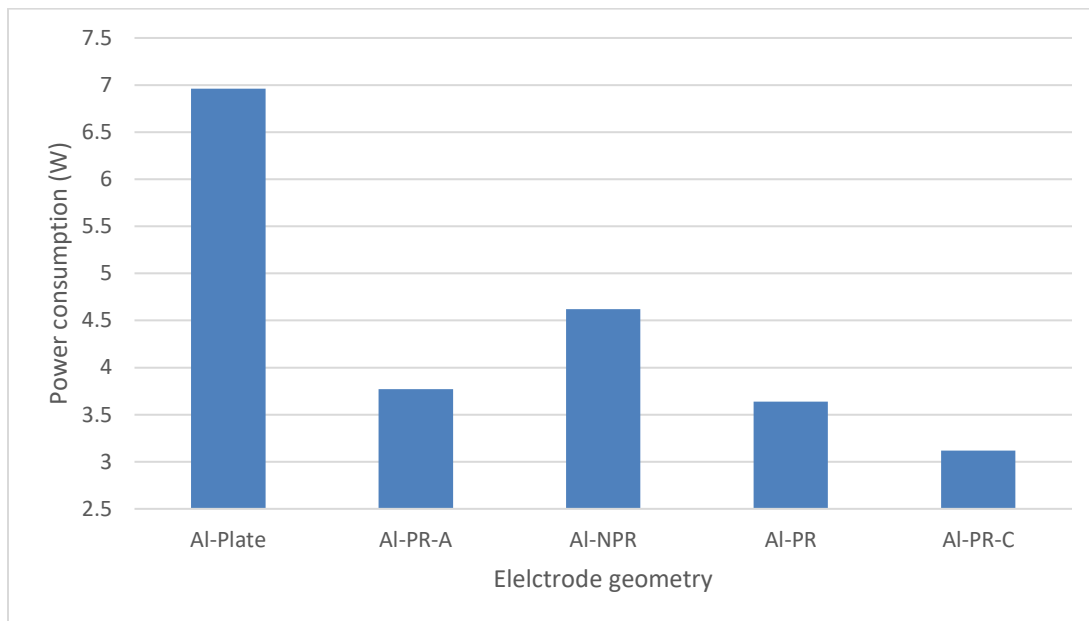
| Electrode geometry | Initial potential difference (V) | Final potential difference (V) | Power consumption (W) |
|--------------------|----------------------------------|--------------------------------|-----------------------|
| Al-Plate           | 2.5                              | 8.2                            | 6.96                  |
| Al-PR-A            | 2.6                              | 3.2                            | 3.77                  |
| Al-NPR             | 2.5                              | 4.6                            | 4.62                  |
| Al-PR              | 2.5                              | 3.1                            | 3.64                  |
| Al-PR-C            | 2.4                              | 2.4                            | 3.12                  |

Figure 19 shows that potential difference between anode and cathode increased in all geometries except for the perforated cathode and non-Perforated anode. This proves the assumption that allowing air to flow from the cathode perforations minimizes passivation, which in turn improves the performance of the reactor. It was also noticed that there is a sharp increase in potential difference when aluminum plate electrodes were used. When both non-perforated anode and cathode were used, the potential difference also increased significantly as the cathode passivation was not eliminated by any means. The performance of the two setups, perforated anode only and both perforated electrodes, was almost identical. When only the anode was perforated, cathode passivation was not eliminated and the anode was not in complete contact with the solution due to the intense air flowrate

being bubbled along the anode surface; this caused a slight increase in potential difference due to cathode passivation but the power consumption was not high because of the partial isolation of anode. On the other hand, when both electrodes were perforated, the air flow rate was divided between the electrodes and passivation was not eliminated effectively. Figure 20 shows the average power consumption for all geometries and proves that Al-PR-C consumes the least power compared to other geometries.



*Figure 19:* Initial and final potential difference for different electrode geometries. PD is potential difference.



*Figure 20:* Power consumption for different electrode geometries at constant current of 1,3 A.

Figure 21 shows the passive layer formed on cathode surface using different electrode geometries. It could be seen that both aluminum plate electrodes and non-perforated cylindrical electrodes were heavily passivated with a thick continuous white layer. On the other hand, when using both perforated electrodes, the passive layer was peeling off and not attached to the cathode surface due to the effect of air flowing along the cathode surface. Finally, when air was bubbled only from the cathode surface, passivation was minimum and the cathode surface was relatively clean since the intensity of air bubbles is higher. Therefore, perforated cathode and non-perforated anode was selected as the



optimum electrode geometry and the next step is optimizing the operating conditions using statistical analysis.

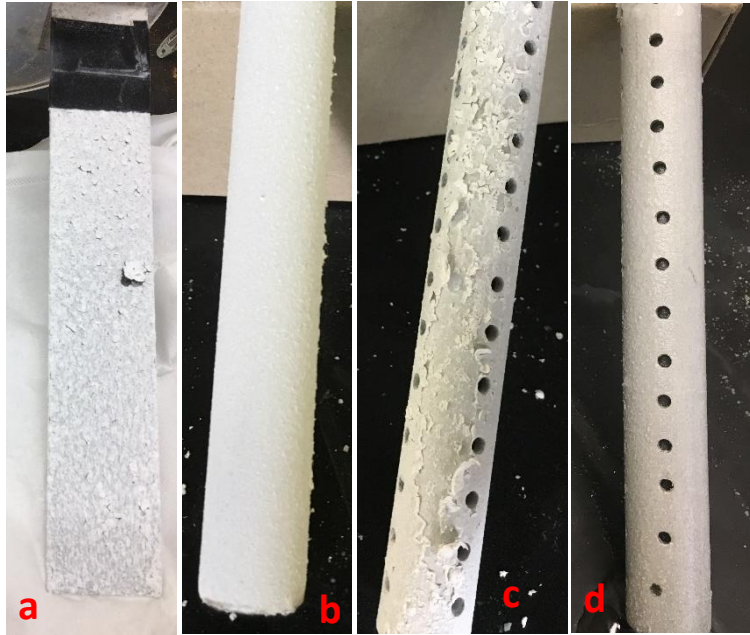


*Figure 21:* Cathode passivation with different electrode geometries: a (Al-Plate), b( Al-NPR), c(Al-PR), d(Al-PR-C)

### **4.3 Optimization of selected geometry**

#### **4.3.1 Theory and steps of Response Surface Methodology (RSM)**

Now that the cell design and the optimum electrode geometry are selected, optimizing the operating conditions is the next step. In order to optimize the performance of the selected electrode geometry, several factors and operating parameters, such as pH, current density

and air flowrate must be considered . Although optimization could be carried out using a one-variable-at-a-time method, where one parameter is changed while keeping the others constant, this approach wouldn't account for any possible interaction between the parameters. Moreover, this method is time consuming as it may lead to performing more experiments than required as well as consuming more reagents and materials. Therefore, RSM, which is a multivariate statistical technique, is used to for this task to overcome these limitations. RSM combines mathematical and statistical techniques that are based on fitting a polynomial function to the experimental data. The predicted polynomial must describe the effect of several independent variables on a specific response. The steps to perform RSM are listed below:

- 1- Screening of independent variables and selecting the most important factors with major effect on the response.
- 2- Selecting the experimental domain, which is defined by the maximum and minimum limits of each factor (independent variable).
- 3- Selecting the proper experimental design which could be first order models where the response must be fitted to the following equation:

$$y = \beta_0 \sum_{i=1}^k \beta_i X_i + \varepsilon \quad (11)$$

Where y is the response,  $\beta_0$  is a constant, k is the number of variables,  $\beta_i$  represents the coefficients of the linear parameters,  $X_i$  are the variables and  $\varepsilon$  is the residual expressed as the difference between the calculated and experimental results.

If the response could not be fitted to the previous equation, then second order response surface models must be used to account for the curvature and interaction between variables.

Examples of second order designs are: Box- Behnken design, central composite design and three-level factorial design. The second order polynomial is expressed as follows:

$$y = \beta_0 + \sum_{i=1}^k \beta_i X_i + \sum_{i=1}^k \beta_{ii} X_i^2 + \sum_{1 \leq i < j \leq k} \beta_{ij} X_j X_i + \varepsilon \quad (12)$$

Where  $\beta_{ii}$  is the coefficient of quadratic parameters and  $\beta_{ij}$  is the coefficient of interacting parameters.

- 4- Choosing the desired response which is dependent on the factors (independent variables).
- 5- Analyzing the response surface design to get the polynomial equation and the interaction between parameters.
- 6- If desired, the response optimizer tool may be used to predict the optimum response as a function of the experimental factors.

#### **4.3.2 RSM results and discussions**

Minitab software was used to perform RSM analysis following the steps mentioned above. Central composite experimental design was selected with three continuous factors: current density, air flowrate and pH of the water. The maximum and minimum values for each factor are given in Table 14.

Table 14: Maximum and minimum levels of experimental factors

| Factor          | Minimum               | Maximum               |
|-----------------|-----------------------|-----------------------|
| Current Density | 10 mA/cm <sup>2</sup> | 20 mA/cm <sup>2</sup> |
| Air flowrate    | 10 SCFH               | 20 SCFH               |
| pH              | 4                     | 10                    |

In case of the central composite design, each of the three factors is studied in five coded levels (- $\alpha$ , -1, 0, +1, + $\alpha$ ). Where 0 is the midpoint, -1 is the minimum level, +1 is the maximum level, - $\alpha$  and + $\alpha$  are two additional levels outside the maximum and minimum range of the variables.  $\alpha$  values are obtained from the following equation:

$$\alpha = 2^{\frac{k-p}{4}} \quad (13)$$

For the selected design, 20 experiments were generated and performed according to the specified run order. The responses were selected as TOC, O&G and TPH percent reduction. Table 15 summarizes the experimental design and the responses.

*Table 15:* Summary of experimental design and responses in terms of percent reduction in TOC, TPH and O&G.

| Run Order | CD    | AF    | pH | TOC   | TPH  | O&G  |
|-----------|-------|-------|----|-------|------|------|
| 1         | 15    | 15    | 7  | 98.1  | 98.2 | 97.4 |
| 2         | 15    | 15    | 7  | 98    | 98.4 | 100  |
| 3         | 15    | 15    | 7  | 98.4  | 99.5 | 100  |
| 4         | 10    | 10    | 4  | 89    | 95.2 | 95.3 |
| 5         | 15    | 23.40 | 7  | 97    | 99.4 | 88.2 |
| 6         | 15    | 15    | 7  | 98.3  | 98.8 | 100  |
| 7         | 23.40 | 15    | 7  | 97.9  | 95   | 99.5 |
| 8         | 15    | 15    | 2  | 86.14 | 91   | 95.6 |
| 9         | 15    | 15    | 7  | 97.7  | 97.9 | 95.2 |
| 10        | 20    | 10    | 4  | 97.1  | 99.4 | 97.3 |
| 11        | 15    | 6.59  | 7  | 97.8  | 98.6 | 94   |
| 12        | 20    | 20    | 4  | 95.2  | 99.1 | 98.3 |
| 13        | 10    | 20    | 4  | 96.5  | 98.3 | 97.2 |
| 14        | 15    | 15    | 12 | 0     | N.A  | N.A  |
| 15        | 20    | 20    | 10 | 0     | N.A  | N.A  |
| 16        | 10    | 10    | 10 | 0     | N.A  | N.A  |
| 17        | 10    | 20    | 10 | 0     | N.A  | N.A  |
| 18        | 20    | 10    | 10 | 0     | N.A  | N.A  |
| 19        | 15    | 15    | 7  | 98.1  | 99.1 | 99.8 |
| 20        | 6.59  | 15    | 7  | 97.8  | 99.6 | 98.1 |

N.A: Not Applicable. CD is current density (mA/cm<sup>2</sup>); AF is air flow rate (SCFH)

It could be seen from Table 15 that all experiments within the pH range of 2-7 gave excellent responses unlike experiments 14-18 with pH of 10 and 12. In order to increase the pH to 10 or 12, concentrated sodium hydroxide solution was carefully introduced dropwise. It was noticed that the pH of the solution initially increases rapidly with adding NaOH until the pH is around 9. When trying to increase the pH beyond that value, the solution acted as a buffer, consuming considerable amounts of NaOH without a change in pH. As more NaOH is added and the desired pH is reached (10 or 12), it was noticed that the solution became milky and very viscous. When oil was added and mixed thoroughly with the homogenizer, it was observed that oil droplets immediately dissolve and disappear within the solution. The experiments were then run each at the specified conditions; however, the solution was very viscous that air mixing was insufficient. The aeration could only be noticed around the cathode but the solution around the anode was stagnant. When the treated sample is left to allow the sludge to precipitate, No settling was observed even after 24 hrs; the solution remained viscous and turbid as if the sample was not treated at all (Figure 22).



*Figure 22: Untreated sample (left) and treated sample (right) at pH 10*

To confirm whether the experiments were successful or not, samples were taken for TOC, TPH and O&G analysis. For TOC analysis, the TOC content before and after the treatment was unchanged, which proves that electrocoagulation was not effective at these conditions. For TPH and O&G analysis, the extraction was not possible as the organic solvents used for liquid-liquid extraction were mixed with the sample and no separation could be seen. Therefore no data for TPH or O&G could be obtained for experiments with pH of 10-12. A possible explanation for the failure of EC at these conditions is that the solution was very viscous that metal ions could not flow within the solution. The cathode and anode were partially isolated by the viscous solution and the lack of mixing. In real life, the pH of produced water could never exceed 9; therefore, these conditions were not practical.

To identify the compounds that are formed with increasing the pH, the sample was dried and the sludge was analyzed using XRD. The results show that increasing the pH leads to precipitating magnesium hydroxides along with calcium carbonate and aluminum hydroxides, which are characterized by their white color and low solubility in water (Figure 23). This explains the milky color of samples with high pH. It was also reported in the literature that increasing the pH is frequently used to recover magnesium from brine as it leads to precipitating magnesium hydroxides. Moreover, mixing oil with sodium hydroxide leads to soap formation (Saponification process); this was observed during the EC experiments as the solution was foaming as a result of air bubbling. When the sample was dried, the sludge was a white creamy/ soapy material and didn't dry into a powder form due to the presence of oil.

Since the TPH and O&G response for the five experiments with high pH were missing, their response could not be analyzed using Minitab. The response of TOC only was analyzed and the removal percent was set to zero for all the five experiments with high pH. The lack of fit was significant which means that the predicted polynomial is not well fitted to the experimental data. This is due to the sudden drop in the response to zero in five experiments compared to 85+ with the other 15 experiments. In order to solve the lack of fit issue, two options were considered: modifying the design and considering pH as a non-continuous factor with specific levels or eliminating the five experiments with zero response and analyzing the response of the remaining 15 experiments. For the first option, only the response of TOC was analyzed as TPH and O&G didn't have any response at high pH. Five separate level of pH were studied: 2, 4, 7, 10 and 12, and five different polynomials for each pH level were obtained to predict the response as a function of the



other two continuous factors (CD and AF). Although this modification solved the lack of fit issue, it was not favorable as it restricts the pH to specific values and excludes any pH value in between. Table 16 summarizes the TOC polynomials and optimum conditions using the first scenario.

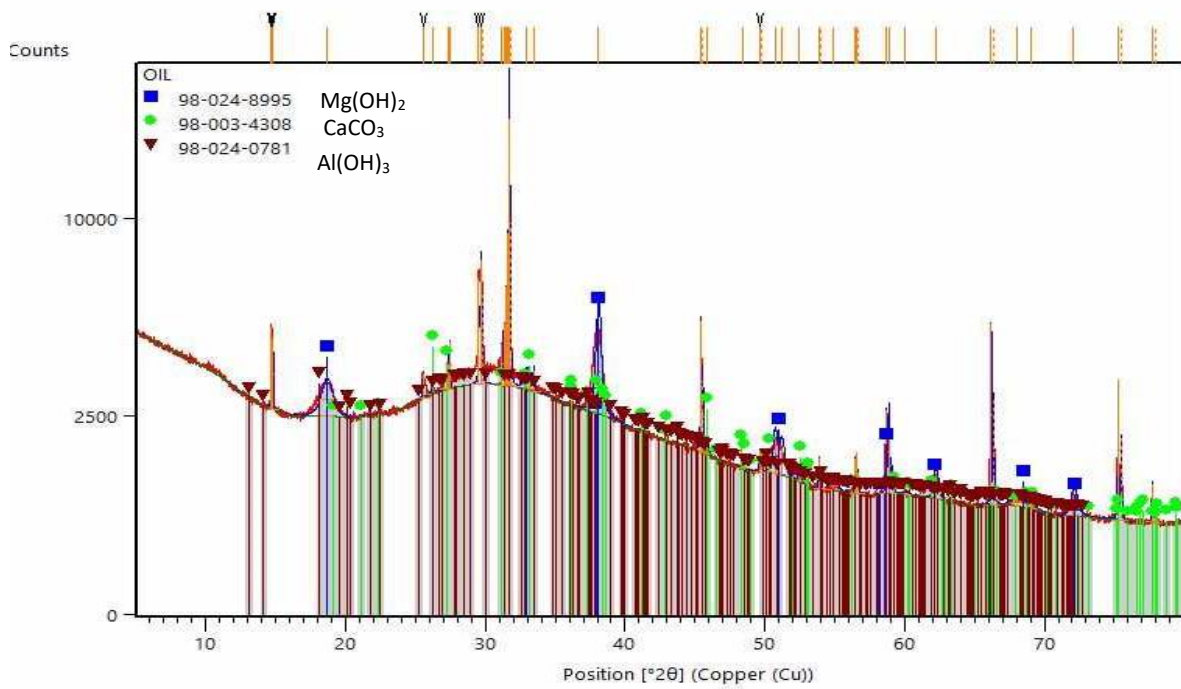
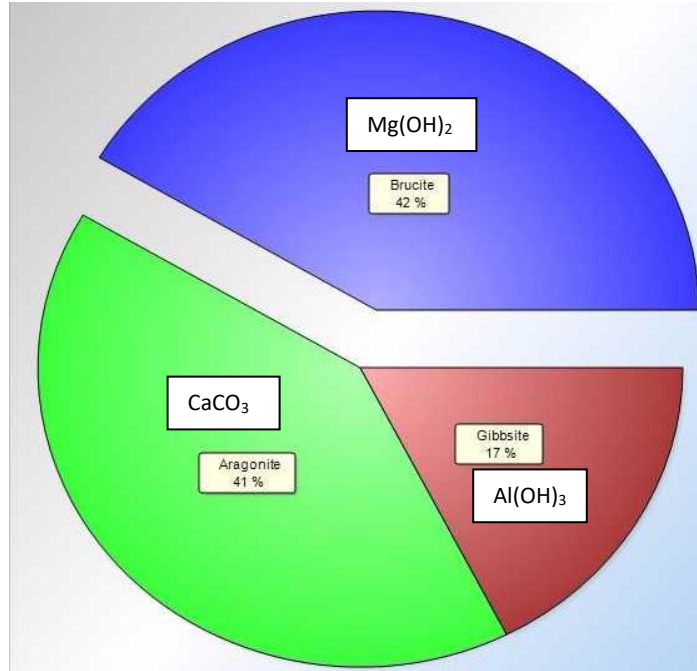


Figure 23: XRD results for PW sludge at pH 10

Table 16: TOC response and optimum conditions, first scenario

| <b>pH</b>   | <b>TOC response</b>   |
|-------------|---|
| <b>1.95</b> | $TOC = 80.06 + 0.366 CD + 0.445 AF - 0.00354 CD*CD - 0.00707 AF*AF - 0.01650 CD*AF$ |
| <b>4</b>    | $TOC = 90.11 + 0.366 CD + 0.445 AF - 0.00354 CD*CD - 0.00707 AF*AF - 0.01650 CD*AF$ |
| <b>7</b>    | $TOC = 92.02 + 0.366 CD + 0.445 AF - 0.00354 CD*CD - 0.00707 AF*AF - 0.01650 CD*AF$ |
| <b>10</b>   | $TOC = -5.81 + 0.366 CD + 0.445 AF - 0.00354 CD*CD - 0.00707 AF*AF - 0.01650 CD*AF$ |
| <b>12</b>   | $TOC = -6.08 + 0.366 CD + 0.445 AF - 0.00354 CD*CD - 0.00707 AF*AF - 0.01650 CD*AF$ |

| <b>Optimum conditions</b>         |                     |              |
|-----------------------------------|---------------------|--------------|
| <b>CD: 23.41 A/cm<sup>2</sup></b> | <b>AF: 6.6 SCFH</b> | <b>pH: 7</b> |

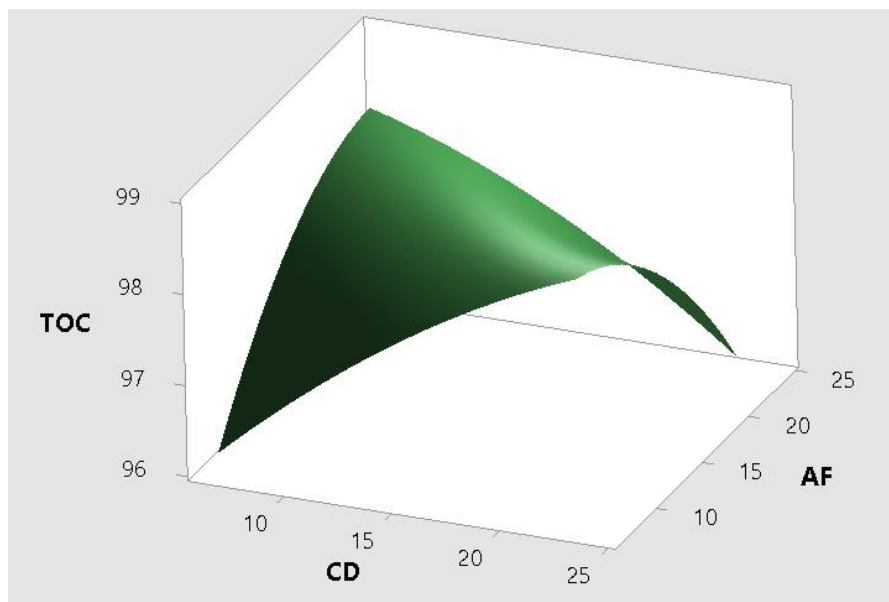


Figure 24: Surface plot of TOC versus CD and AF at pH of 7

For the second option, the five experiments with zero response were eliminated and the response was analyzed for the remaining experiments. Using this technique is not only more realistic (for pH range of 2-7), but also more favorable, as it would allow for the inclusion of other responses (TPH and O&G). The results of this scenario are summarized in Table 17.

*Table 17: TOC, TPH and O&G responses and optimum conditions for second scenario*

| <b>pH</b>                 | <b>TOC, TPH and O&amp;G responses</b>  |                      |              |
|---------------------------|--|----------------------|--------------|
| <b>1.95-7</b>             | $\text{TOC} = 26.33 + 2.301 \text{ CD} + 2.424 \text{ AF} + 11.220 \text{ pH} - 0.00354 \text{ CD} \cdot \text{CD} - 0.00990 \text{ AF} \cdot \text{AF} \\ - 0.6188 \text{ pH} \cdot \text{pH} - 0.09400 \text{ CD} \cdot \text{AF} - 0.1114 \text{ CD} \cdot \text{pH} - 0.1092 \text{ AF} \cdot \text{pH}$ |                      |              |
|                           | $\text{O\&G} = 46.2 + 0.36 \text{ CD} + 4.17 \text{ AF} + 7.56 \text{ pH} + 0.0009 \text{ CD} - 0.1080 \text{ AF} \cdot \text{AF} \\ - 0.461 \text{ pH} \cdot \text{pH} - 0.0090 \text{ CD} \cdot \text{AF} - 0.0239 \text{ CD} \cdot \text{pH} - 0.1633 \text{ AF} \cdot \text{pH}$                         |                      |              |
|                           | $\text{TPH} = 49.55 + 2.031 \text{ CD} + 0.625 \text{ AF} + 10.80 \text{ pH} - 0.01909 \text{ CD} \cdot \text{CD} + 0.00495 \text{ AF} \cdot \text{AF} \\ - 0.6930 \text{ pH} \cdot \text{pH} - 0.0340 \text{ CD} \cdot \text{AF} - 0.1745 \text{ CD} \cdot \text{pH} - 0.0308 \text{ AF} \cdot \text{pH}$   |                      |              |
| <b>Optimum conditions</b> |  |                      |              |
|                           | <b>CD: 17 A/cm<sup>2</sup></b>   | <b>AF: 15.5 SCFH</b> | <b>pH: 6</b> |

Figures 26, 27 and 28 show the surface plots for TOC, O&G and TPH responses. Since pH is considered as a continuous factor in scenario 2, the optimum conditions are predicted at a pH of 6, CD of 17 A/cm<sup>2</sup> and AF of 15.5 SCFH (Figure 29). To validate the accuracy of the generated polynomials, one experiment was carried out at the optimum conditions and analyzed for the percent reduction of TOC, TPH and O&G. The experimental values were

compared to the predicted response from the polynomials and the error was calculated. Table 18 summarizes the predicted response, experimental response and error for each of the three parameters.

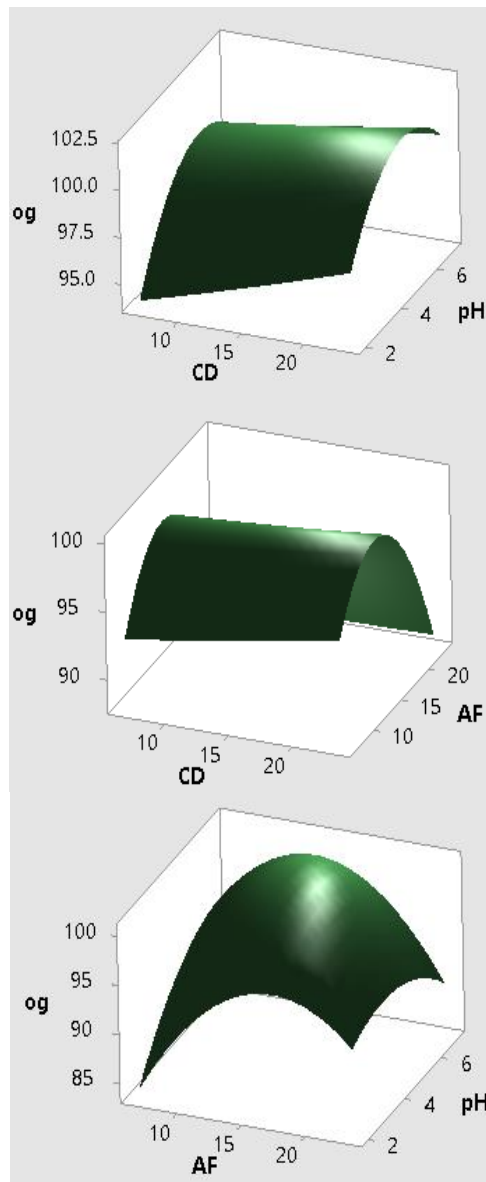


Figure 25: Surface plots for O&G response

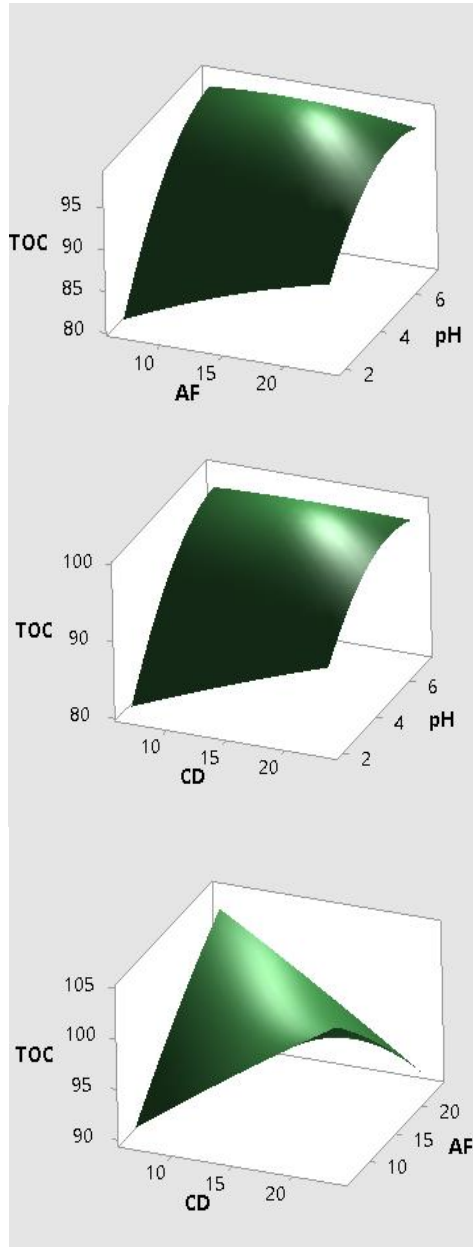


Figure 26: Surface plots for TOC response

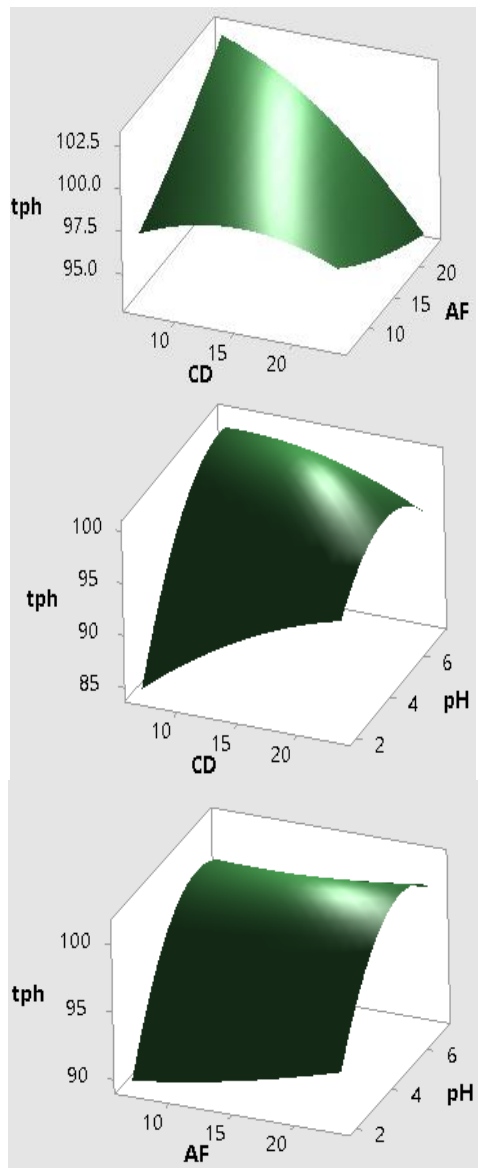


Figure 27: Surface plots for TPH response

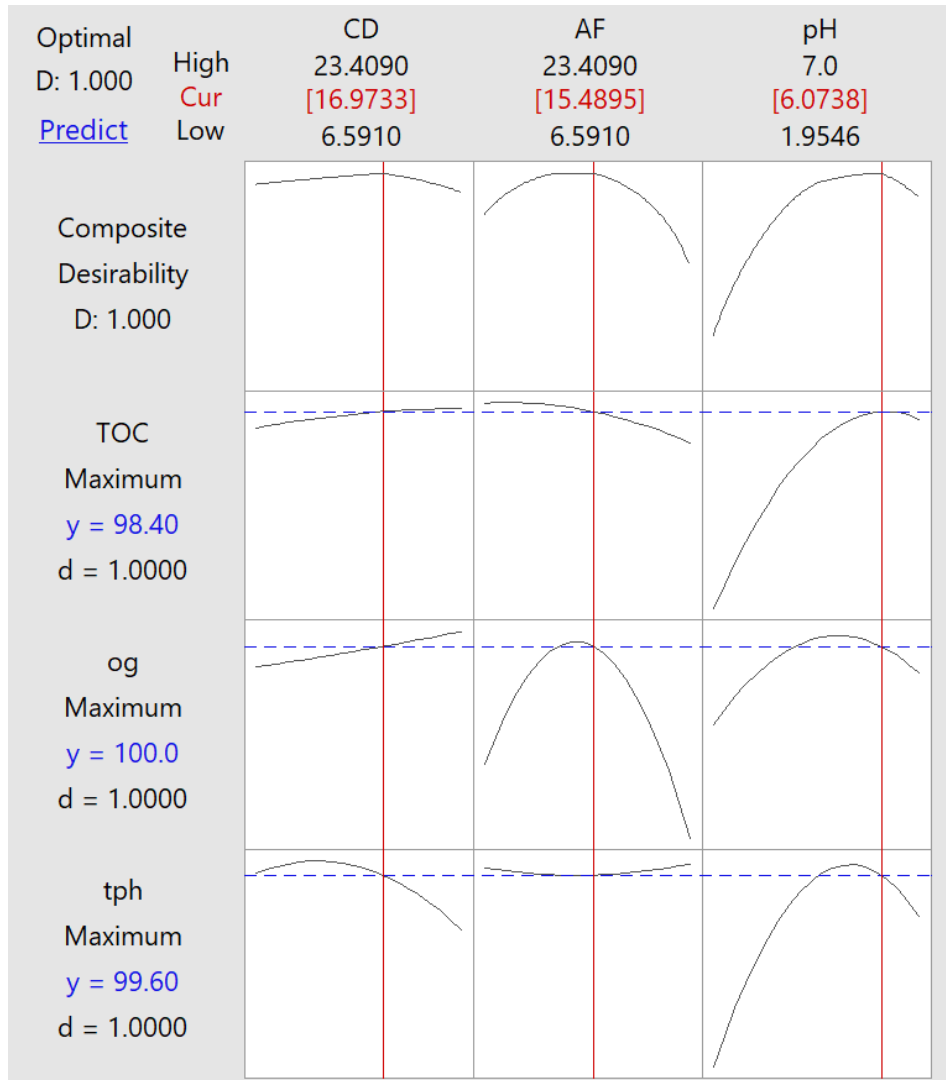


Figure 28: Optimum conditions for second scenario



*Table 18:* Predicted response versus experimental response at optimum conditions

| Response | Predicted | Experimental | Error |
|----------|-----------|--------------|-------|
| TOC      | 98.4 %    | 96.4 %       | 2 %   |
| TPH      | 99.6 %    | 99.1 %       | 0.5 % |
| O&G      | 100 %     | 100 %        | 0 %   |

#### **4.4 Continuous mode of operation**

The last step of this study was to operate the system in a continuous mode at the optimum conditions and observe the effect of aeration on reducing cathode passivation. Since operating the system in a batch mode for 30 minutes gave excellent results, the residence time was selected as 30 minutes and the water flowrate was set at 63.3 mL/min. The continuous experiment was run for 90 minutes and samples were taken every 10 minutes from the reactor outlet. The samples were analyzed for TOC and the removal percent was plotted against time to determine the time taken to reach steady state (Figure 30). The potential difference and power consumption were also monitored to observe the effect of passivation on the system performance. Table 19 summarizes the TOC removal percent, potential difference and power consumption versus time.

*Table 19:* TOC removal percent, potential difference and power consumption versus time

| <b>Time (min)</b> | <b>TOC removal<br/>percent</b> | <b>Potential difference<br/>(V)</b> | <b>Power consumption (W)</b> |
|-------------------|--------------------------------|-------------------------------------|------------------------------|
| <b>0</b>          | 0 %                            | 2.47                                | 3.46                         |
| <b>10</b>         | 12.8%                          | 2.45                                | 3.43                         |
| <b>20</b>         | 91.7%                          | 2.45                                | 3.43                         |
| <b>30</b>         | 94.3%                          | 2.46                                | 3.44                         |
| <b>40</b>         | 94.7%                          | 2.45                                | 3.43                         |
| <b>50</b>         | 95.8%                          | 2.44                                | 3.42                         |
| <b>60</b>         | 95%                            | 2.43                                | 3.40                         |
| <b>70</b>         | 95.6%                          | 2.43                                | 3.40                         |
| <b>80</b>         | 95.8%                          | 2.46                                | 3.44                         |
| <b>90</b>         | 96.8%                          | 2.5                                 | 3.50                         |

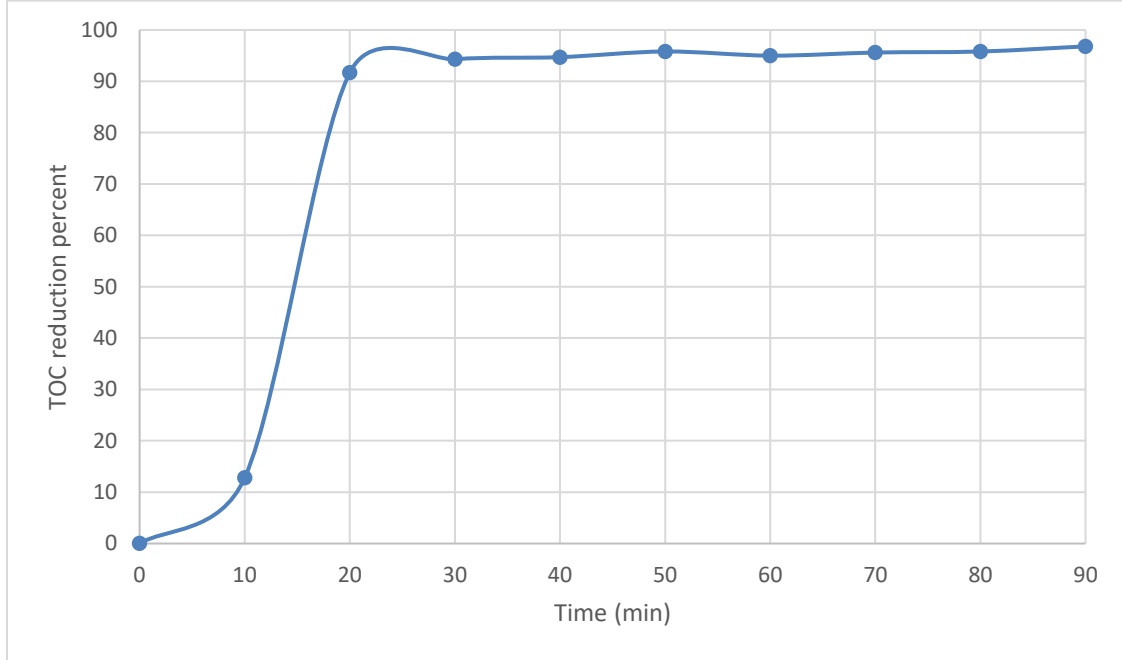


*Figure 29: TOC reduction percent versus time for continuous operation*

Figure 30 shows that steady state is reached after 30 minutes of operation, where the removal percent was almost constant for the remaining 60 minutes. To prove whether the new reactor design is effective in reducing passivation and eliminating the effect of passivation on system performance, the potential difference and power consumption were also plotted versus time

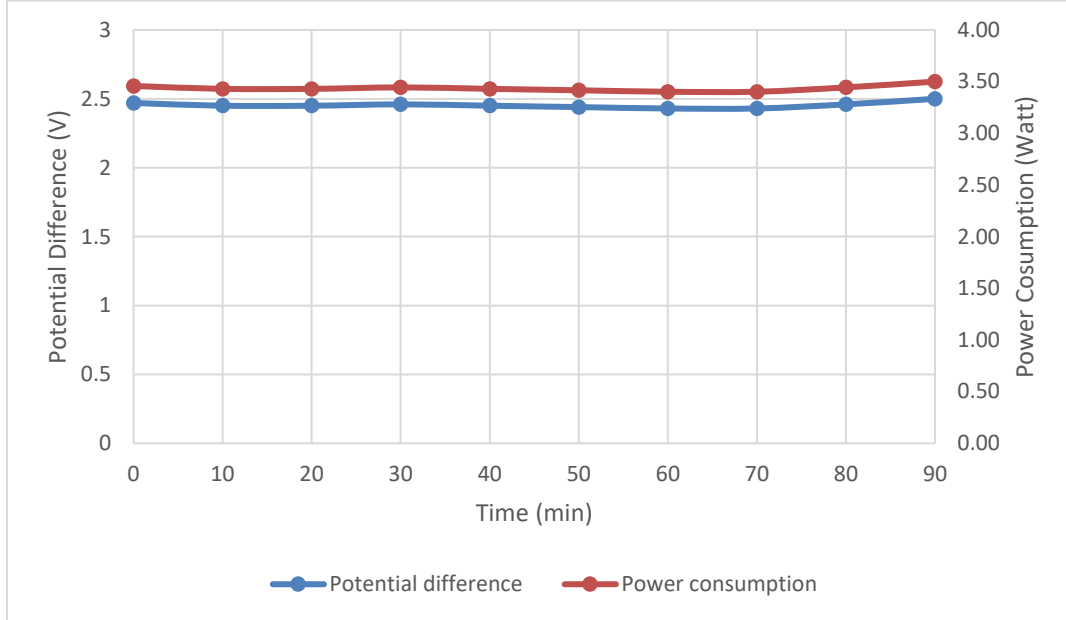


*Figure 30:* Potential difference and power consumption versus time for continuous operation

Figure 31 shows that the potential difference and power consumption were almost constant during the whole treatment time. This proves that allowing air to flow from cathode perforations at high flowrate eliminates the effect of passivation on the system performance. Air bubbles were acting as a cleansing mechanism as well as a mixing tool at the same time.

Figure 32 shows that the cathode was slightly passivated after 90 minutes of operation and the passive layer was peeling off easily and not attached to the cathode surface. These results show major improvement when compared to the system performance with

aluminum plate electrodes. When the system was operated for just 30 minutes in a batch mode using aluminum plate electrodes, the potential difference and power consumption increased significantly (Figure 17).



*Figure 31: Cathode passivation after 90 minutes of continuous operation*

The final removal percent for TOC, TPH and O&G with continuous operation for 90 minutes are summarized in Table 20.

*Table 20:* Summary of TOC, TPH and O&G removal after continuous operation

| Parameter | Removal percent |
|-----------|-----------------|
| TOC       | 96.8 %          |
| TPH       | 97.9 %          |
| O&G       | 94.6 %          |

## **Chapter 5: Research findings and conclusions**

This chapter highlights the main findings and contribution of the research work. Knowing that produced water from oil and gas industries is becoming a global concern due to its complex composition and large volumes generated daily, there has been an increased interest in produced water research recently. Several produced water treatment methods ranging from biological, chemical, physical and electrochemical technologies are employed worldwide. This research focuses on an electrochemical technology known as Electrocoagulation, which is considered a green technology, and possesses several advantages over traditional produced water treatment methods, such as generating less sludge, eliminating chemical additives and the capability of treating oily water. As a first step, the literature was studied extensively to assess the status of the technology and highlight the gap in existing research. This step revealed that Electrocoagulation technology was tested for various types of wastewaters and proven to be effective. However, the technology is not yet mature enough to be employed as a reliable wastewater treatment technology. Most of the published literature focused on proving the effectiveness of Electrocoagulation to treat wastewaters in a basic batch mode of operation without presenting a systematic approach for reactor design and scale up. This was achieved by altering the operating conditions and customizing them to different types of wastewaters. This current study, however, focused on designing a new reactor that would overcome cathode passivation, a major limitation of Electrocoagulation technology, regardless of the operating conditions. A perforated hollow cylindrical cathode was used with compressed air allowed to flow from cathode

perforations to clean the electrode and provide sufficient mixing. The new reactor design was tested for treating synthetic produced water and the results were compared to basic electrocoagulation setups with plate electrodes. The novel reactor was found to be more efficient in treating produced water and minimizing cathode passivation. To further optimize the performance, statistical analysis was used and the optimum operating conditions was obtained. The system was then run at optimum conditions in a continuous mode of operation and the cathode passivation was monitored. It was observed that cathode passivation was minimized significantly and the system performance was stable even with continuous operation for 90 minutes. In conclusion, this study came up with a novel reactor design that proved to be effective in treating produced water and showed enhanced performance compared to simple electrocoagulation setup regardless of operating conditions.



## **Chapter 6: Future work**

Since obtaining real produced water samples was not possible for this research work, the effect of corrosion inhibitors on the performance of electrocoagulation was not studied. Corrosion inhibitors are normally added to injection water to protect the wellhead tubing from corrosion and they come along with produced water. Electrocoagulation is not effective without anode dissolution due to the applied current, which is also known as corrosion. The presence of corrosion inhibitors is expected to deteriorate the system performance. Therefore, future research should study the effect of corrosion inhibitors on electrocoagulation.

Future research should also consider different electrode arrangements such as parallel and series connections that would play a major role in reactor scale up for industrial applications.

Integrating electrocoagulation with existing technologies is another crucial aspect that must be considered in future research. Several authors reported that using electrocoagulation technology as a pretreatment of existing mature technologies not only enhances the treatment of wastewaters, but also protects the existing equipment and increases their lifetime.

## References

- [1] M. El-Naas and D. Moussa, "Electrochemical technologies for produced water treatment," *Materials Research Foundations*, vol. 16.
- [2] D. T. Moussa, M. H. El-Naas, M. Nasser, and M. J. Al-Marri, "A comprehensive review of electrocoagulation for water treatment: Potentials and challenges," *Journal of Environmental Management*, vol. 186, Part 1, pp. 24-41, 1/15/ 2017.
- [3] K. Guerra, K. Dahm, and S. Dundorf, "Oil and Gas Produced Water Management and Beneficial Use in the Western United States: Science and Technology Program Report No. 157," *US Department of the Interior, Bureau of Reclamation, Denver, CO*, 2011.
- [4] J. Neff, K. Lee, and E. M. DeBlois, "Produced water: overview of composition, fates, and effects," in *Produced water*: Springer, 2011, pp. 3-54.
- [5] M. E. Mantell, "Produced water reuse and recycling challenges and opportunities across major shale plays," in *Proceedings of the technical workshops for the hydraulic fracturing study: water resources management. EPA*, 2011, vol. 600, pp. 49-57.
- [6] C. C. d. Almeida, P. R. F. d. Costa, M. J. d. M. Melo, E. V. d. Santos, and C. A. Martínez-Huitle, "Application of Electrochemical Technology for Water Treatment of Brazilian Industry Effluents," *Journal of the Mexican Chemical Society*, vol. 58, no. 3, pp. 276-286, 2014.
- [7] R. T. Duraisamy, A. H. Beni, and A. Henni, *State of the Art Treatment of Produced Water (Water Treatment)*. 2013.

- [8] E. T. Igunnu and G. Z. Chen, "Produced water treatment technologies," *International Journal of Low-Carbon Technologies*, p. cts049, 2012.
- [9] A. Maddocks, R. Young, and P. Reig. (2015, August, 19). *Ranking the World's Most Water-Stressed Countries in 2040*. Available:  
<https://www.wri.org/blog/2015/08/ranking-world%E2%80%99s-most-water-stressed-countries-2040>
- [10] M. Abdou *et al.*, "Finding value in formation water," *Oilfield Review*, vol. 23, no. 1, pp. 24-35, 2011.
- [11] G. W. Miller, "Integrated concepts in water reuse: managing global water needs," *Desalination*, vol. 187, no. 1, pp. 65-75, 2006.
- [12] K. B. Gregory, R. D. Vidic, and D. A. Dzombak, "Water management challenges associated with the production of shale gas by hydraulic fracturing," *Elements*, vol. 7, no. 3, pp. 181-186, 2011.
- [13] D. L. Shaffer, L. H. Arias Chavez, M. Ben-Sasson, S. Romero-Vargas Castrillón, N. Y. Yip, and M. Elimelech, "Desalination and reuse of high-salinity shale gas produced water: drivers, technologies, and future directions," *Environmental science & technology*, vol. 47, no. 17, pp. 9569-9583, 2013.
- [14] R. Kimball, "Key considerations for frac flowback/produced water reuse and treatment," in *NJWEA Annual Conference*, 2011, pp. 9-13.
- [15] Z. Khatib and P. Verbeek, "Water to value-produced water management for sustainable field development of mature and green fields," *Journal of Petroleum Technology*, vol. 55, no. 01, pp. 26-28, 2003.

- [16] U. N. E. a. S. C. f. W. Asia, *Waste-water Treatment Technologies: A General Review*. United Nations, Economic and Social Commission for Western Asia, 2003.
- [17] E. T. Igunnu and G. Z. Chen, "Produced water treatment technologies," *International Journal of Low-Carbon Technologies*, vol. 9, no. 3, pp. 157-177, 2012.
- [18] G. Chen, "Electrochemical technologies in wastewater treatment," *Separation and Purification Technology*, vol. 38, no. 1, pp. 11-41, 7/15/ 2004.
- [19] G. Chen and Y.-T. Hung, "Electrochemical Wastewater Treatment Processes," in *Advanced Physicochemical Treatment Technologies*, L. K. Wang, Y.-T. Hung, and N. K. Shamas, Eds. Totowa, NJ: Humana Press, 2007, pp. 57-106.
- [20] V. Kuokkanen, T. Kuokkanen, J. Ramo, and U. Lassi, "Recent applications of electrocoagulation in treatment of water and wastewater- A review," *Scientific research*, vol. 3, no. 2, pp. 89-121, 2013.
- [21] H. A. Moreno C *et al.*, "Electrochemical Reactions for Electrocoagulation Using Iron Electrodes," *Industrial & Engineering Chemistry Research*, vol. 48, no. 4, pp. 2275-2282, 2009/02/18 2009.
- [22] P. K. Holt, G. W. Barton, M. Wark, and C. A. Mitchell, "A quantitative comparison between chemical dosing and electrocoagulation," *Colloids and Surfaces A: Physicochemical and Engineering Aspects*, vol. 211, no. 2-3, pp. 233-248, 12/3/ 2002.
- [23] S. Mhatre *et al.*, "Electrostatic phase separation: A review," *Chemical Engineering Research and Design*, vol. 96, pp. 177-195, 4// 2015.

- [24] D. Ghernaout, M. W. Naceur, and B. Ghernaout, "A review of electrocoagulation as a promising coagulation process for improved organic and inorganic matters removal by electrophoresis and electroflotation," *Desalination and water treatment*, vol. 28, pp. 287-320, 2011.
- [25] M. Vepsäläinen, "Electrocoagulation in the treatment of industrial waters and wastewaters," Doctor of Science (Technology), Department of Energy and Environmental Technology, Lappeenranta University of Technology, Mikkeli, Finland, VTT science 19, 2012.
- [26] O. Duman and S. Tunç, "Electrokinetic and rheological properties of Na-bentonite in some electrolyte solutions," *Microporous and Mesoporous Materials*, vol. 117, no. 1-2, pp. 331-338, 2009.
- [27] T. F. Tadros, "Prevention of formation of dilatant sediments in suspension concentrates," *Colloids and Surfaces*, vol. 18, no. 2-4, pp. 427-438, 1986.
- [28] T. F. Tadros, "Disperse systems in pesticidal formulations," *Advances in Colloid and Interface Science*, vol. 32, no. 2-3, pp. 205-234, 1990.
- [29] M. S. Nasser and A. E. James, "Settling and sediment bed behaviour of kaolinite in aqueous media," *Separation and Purification Technology*, vol. 51, no. 1, pp. 10-17, 2006.
- [30] M. S. Nasser and A. E. James, "The effect of polyacrylamide charge density and molecular weight on the flocculation and sedimentation behaviour of kaolinite suspensions," *Separation and Purification Technology*, vol. 52, no. 2, pp. 241-252, 2006.

- [31] M. S. Nasser and A. E. James, "Numerical simulation of the continuous thickening of flocculated kaolinite suspensions," *International Journal of Mineral Processing*, vol. 84, no. 1–4, pp. 144-156, 2007.
- [32] C. Chassagne, F. Mietta, and J. C. Winterwerp, "Electrokinetic study of kaolinite suspensions," *Journal of Colloid and Interface Science*, vol. 336, no. 1, pp. 352-359, 2009.
- [33] D. J. A. Williams and K. P. Williams, "Electrophoresis and zeta potential of kaolinite," *Journal of Colloid and Interface Science*, vol. 65, no. 1, pp. 79-87, 1978.
- [34] M. Y. A. Mollah, P. Morkovsky, J. A. G. Gomes, M. Kesmez, J. Parga, and D. L. Cocke, "Fundamentals, present and future perspectives of electrocoagulation," *Journal of Hazardous Materials*, vol. 114, no. 1–3, pp. 199-210, 10/18/ 2004.
- [35] H. A. Moreno C *et al.*, "Electrochemical Reactions for Electrocoagulation Using Iron Electrodes," *Industrial & Engineering Chemistry Research*, vol. 48, no. 4, pp. 2275-2282, 2009/02/18 2009.
- [36] G. Mouedhen, M. Feki, M. D. P. Wery, and H. F. Ayedi, "Behavior of aluminum electrodes in electrocoagulation process," *Journal of Hazardous Materials*, vol. 150, no. 1, pp. 124-135, 1/15/ 2008.
- [37] M. Kobya, H. Hiz, E. Senturk, C. Aydinler, and E. Demirbas, "Treatment of potato chips manufacturing wastewater by electrocoagulation," *Desalination*, vol. 190, no. 1–3, pp. 201-211, 4/15/ 2006.
- [38] P. Cañizares, M. Carmona, J. Lobato, F. Martínez, and M. A. Rodrigo, "Electrodissolution of Aluminum Electrodes in Electrocoagulation Processes,"

- Industrial & Engineering Chemistry Research*, vol. 44, no. 12, pp. 4178-4185, 2005/06/01 2005.
- [39] M. Y. A. Mollah, R. Schennach, J. R. Parga, and D. L. Cocke, "Electrocoagulation (EC) — science and applications," *Journal of Hazardous Materials*, vol. 84, no. 1, pp. 29-41, 6/1/ 2001.
- [40] M. Kobya and E. Demirbas, "Evaluations of operating parameters on treatment of can manufacturing wastewater by electrocoagulation," *Journal of Water Process Engineering*, vol. 8, pp. 64-74, 12// 2015.
- [41] Y. Demirci, L. C. Pekel, and M. Albaz, "Investigation of different electrode connections in electrocoagulation of textile wastewater treatment," *International journal of electrochemical science*, pp. 2685-2693, 2015.
- [42] V. Khandegar and A. K. Saroha, "Electrocoagulation for the treatment of textile industry effluent – A review," *Journal of Environmental Management*, vol. 128, pp. 949-963, 10/15/ 2013.
- [43] A. K. Golder, A. N. Samanta, and S. Ray, "Removal of Cr<sup>3+</sup> by electrocoagulation with multiple electrodes: Bipolar and monopolar configurations," *Journal of Hazardous Materials*, vol. 141, no. 3, pp. 653-661, 3/22/ 2007.
- [44] D. Ghosh, C. R. Medhi, and M. K. Purkait, "Treatment of fluoride containing drinking water by electrocoagulation using monopolar and bipolar electrode connections," *Chemosphere*, vol. 73, no. 9, pp. 1393-1400, 11// 2008.
- [45] Z.-h. Yang *et al.*, "The behavior of dissolution/passivation and the transformation of passive films during electrocoagulation: Influences of initial pH, Cr(VI)

- concentration, and alternating pulsed current," *Electrochimica Acta*, vol. 153, pp. 149-158, 1/20/ 2015.
- [46] S. Vasudevan, J. Lakshmi, and G. Sozhan, "Effects of alternating and direct current in electrocoagulation process on the removal of cadmium from water," *Journal of Hazardous Materials*, vol. 192, no. 1, pp. 26-34, 8/15/ 2011.
- [47] M. Eyvaz, M. Kirlaroglu, T. S. Aktas, and E. Yuksel, "The effects of alternating current electrocoagulation on dye removal from aqueous solutions," *Chemical Engineering Journal*, vol. 153, no. 1–3, pp. 16-22, 11/1/ 2009.
- [48] H. J. Mansoorian, A. H. Mahvi, and A. J. Jafari, "Removal of lead and zinc from battery industry wastewater using electrocoagulation process: Influence of direct and alternating current by using iron and stainless steel rod electrodes," *Separation and Purification Technology*, vol. 135, pp. 165-175, 10/15/ 2014.
- [49] M. Kobya, E. Gengec, and E. Demirbas, "Operating parameters and costs assessments of a real dyehouse wastewater effluent treated by a continuous electrocoagulation process," *Chemical Engineering and Processing: Process Intensification*.
- [50] E. Gatsios, J. N. Hahladakis, and E. Gidarakos, "Optimization of electrocoagulation (EC) process for the purification of a real industrial wastewater from toxic metals," *Journal of Environmental Management*, vol. 154, pp. 117-127, 5/1/ 2015.
- [51] B. Khaled, B. Wided, H. Béchir, E. Elimame, L. Mouna, and T. Zied, "Investigation of electrocoagulation reactor design parameters effect on the



- removal of cadmium from synthetic and phosphate industrial wastewater," *Arabian Journal of Chemistry*.
- [52] A. Attour, M. Touati, M. Tlili, M. Ben Amor, F. Lopicque, and J. P. Leclerc, "Influence of operating parameters on phosphate removal from water by electrocoagulation using aluminum electrodes," *Separation and Purification Technology*, vol. 123, pp. 124-129, 2/26/ 2014.
- [53] S. Bayar, Y. Ş. Yıldız, A. E. Yılmaz, and Ş. İrdemez, "The effect of stirring speed and current density on removal efficiency of poultry slaughterhouse wastewater by electrocoagulation method," *Desalination*, vol. 280, no. 1–3, pp. 103-107, 10/3/ 2011.
- [54] C. Y. Hu, S. L. Lo, and W. H. Kuan, "Effects of co-existing anions on fluoride removal in electrocoagulation (EC) process using aluminum electrodes," *Water Research*, vol. 37, no. 18, pp. 4513-4523, 11// 2003.
- [55] J. L. Trompette and H. Vergnes, "On the crucial influence of some supporting electrolytes during electrocoagulation in the presence of aluminum electrodes," *Journal of Hazardous Materials*, vol. 163, no. 2–3, pp. 1282-1288, 4/30/ 2009.
- [56] C. Barrera-Díaz, G. Roa-Morales, L. Ávila-Córdoba, T. Pavón-Silva, and B. Bilyeu, "Electrochemical Treatment Applied to Food-Processing Industrial Wastewater," *Industrial & Engineering Chemistry Research*, vol. 45, no. 1, pp. 34-38, 2006/01/01 2006.
- [57] I. Linares-Hernández, C. Barrera-Díaz, G. Roa-Morales, B. Bilyeu, and F. Ureña-Núñez, "Influence of the anodic material on electrocoagulation performance," *Chemical Engineering Journal*, vol. 148, no. 1, pp. 97-105, 5/1/ 2009.

- [58] C. Barrera-Díaz, G. Roa-Morales, L. Ávila-Córdoba, T. Pavón-Silva, and B. Bilyeu, "Electrochemical Treatment Applied to Food-Processing Industrial Wastewater," *Industrial & Engineering Chemistry Research*, vol. 45, no. 1, pp. 34-38, 2006/01/01 2006.
- [59] E. Terrazas, A. Vázquez, R. Briones, I. Lázaro, and I. Rodríguez, "EC treatment for reuse of tissue paper wastewater: Aspects that affect energy consumption," *Journal of Hazardous Materials*, vol. 181, no. 1–3, pp. 809-816, 9/15/ 2010.
- [60] M. Uğurlu, A. Gürses, Ç. Doğar, and M. Yalçın, "The removal of lignin and phenol from paper mill effluents by electrocoagulation," *Journal of Environmental Management*, vol. 87, no. 3, pp. 420-428, 5// 2008.
- [61] O. Abdelwahab, N. K. Amin, and E. S. Z. El-Ashtoukhy, "Electrochemical removal of phenol from oil refinery wastewater," *Journal of Hazardous Materials*, vol. 163, no. 2–3, pp. 711-716, 4/30/ 2009.
- [62] R. Katal and H. Pahlavanzadeh, "Influence of different combinations of aluminum and iron electrode on electrocoagulation efficiency: Application to the treatment of paper mill wastewater," *Desalination*, vol. 265, no. 1–3, pp. 199-205, 1/15/ 2011.
- [63] L. S. Pérez *et al.*, "Oil refinery wastewater treatment using coupled electrocoagulation and fixed film biological processes," *Physics and Chemistry of the Earth, Parts A/B/C*.
- [64] M. H. El-Naas, S. Al-Zuhair, A. Al-Lobaney, and S. Makhlof, "Assessment of electrocoagulation for the treatment of petroleum refinery wastewater," *Journal of Environmental Management*, vol. 91, no. 1, pp. 180-185, 2009.

- [65] J. R. Parga *et al.*, "Characterization of Electrocoagulation for Removal of Chromium and Arsenic  
Chemical Engineering & Technology Volume 28, Issue 5," *Chemical Engineering & Technology*, vol. 28, no. 5, pp. 605-612 Accessed on: 01 Available:  
<http://onlinelibrary.wiley.com/doi/10.1002/ceat.200407035/abstract>
- [66] P. Cañizares, C. Jiménez, F. Martínez, C. Sáez, and M. A. Rodrigo, "Study of the Electrocoagulation Process Using Aluminum and Iron Electrodes," *Industrial & Engineering Chemistry Research*, vol. 46, no. 19, pp. 6189-6195, 2007/09/01 2007.
- [67] X. Xu and X. Zhu, "Treatment of refractory oily wastewater by electro-coagulation process," *Chemosphere*, vol. 56, no. 10, pp. 889-894, 9// 2004.
- [68] D. Lakshmanan, D. A. Clifford, and G. Samanta, "Ferrous and Ferric Ion Generation During Iron Electrocoagulation," *Environmental Science & Technology*, vol. 43, no. 10, pp. 3853-3859, 2009/05/15 2009.
- [69] D. Lakshmanan, D. A. Clifford, and G. Samanta, "Ferrous and Ferric Ion Generation During Iron Electrocoagulation," *Environmental Science & Technology*, vol. 43, no. 10, pp. 3853-3859, 2009/05/15 2009.
- [70] M. Malakootian, H. J. Mansoorian, and M. Moosazadeh, "Performance evaluation of electrocoagulation process using iron-rod electrodes for removing hardness from drinking water," *Desalination*, vol. 255, no. 1-3, pp. 67-71, 5/31/ 2010.

- [71] F. Hussin, F. Abnisa, G. Issabayeva, and M. K. Aroua, "Removal of lead by solar-photovoltaic electrocoagulation using novel perforated zinc electrode," *Journal of Cleaner Production*, vol. 147, pp. 206-216, 2017/03/20/ 2017.
- [72] R. Kamaraj and S. Vasudevan, "Evaluation of electrocoagulation process for the removal of strontium and cesium from aqueous solution," *Chemical Engineering Research and Design*, vol. 93, pp. 522-530, 2015/01/01/ 2015.
- [73] K. Govindan, M. Noel, and R. Mohan, "Removal of nitrate ion from water by electrochemical approaches," *Journal of Water Process Engineering*, vol. 6, pp. 58-63, 2015/06/01/ 2015.
- [74] P. R. Kumar, S. Chaudhari, K. C. Khilar, and S. Mahajan, "Removal of arsenic from water by electrocoagulation," *Chemosphere*, vol. 55, no. 9, pp. 1245-1252, 2004.
- [75] M. H. El-Naas, M. A. Alhaija, and S. Al-Zuhair, "Evaluation of a three-step process for the treatment of petroleum refinery wastewater," *Journal of Environmental Chemical Engineering*, vol. 2, no. 1, pp. 56-62, 3// 2014.
- [76] A. N. Módenes, F. R. Espinoza-Quiñones, F. H. Borba, and D. R. Manenti, "Performance evaluation of an integrated photo-Fenton – Electrocoagulation process applied to pollutant removal from tannery effluent in batch system," *Chemical Engineering Journal*, vol. 197, pp. 1-9, 7/15/ 2012.
- [77] D. R. Manenti *et al.*, "Assessment of a multistage system based on electrocoagulation, solar photo-Fenton and biological oxidation processes for real textile wastewater treatment," *Chemical Engineering Journal*, vol. 252, pp. 120-130, 9/15/ 2014.

- [78] K. Bani-Melhem and E. Smith, "Grey water treatment by a continuous process of an electrocoagulation unit and a submerged membrane bioreactor system," *Chemical Engineering Journal*, vol. 198–199, pp. 201-210, 8/1/ 2012.
- [79] A. Deghles and U. Kurt, "Treatment of tannery wastewater by a hybrid electrocoagulation/electrodialysis process," *Chemical Engineering and Processing: Process Intensification*, vol. 104, pp. 43-50, 6// 2016.
- [80] M. F. Ni'am and F. Othman, "Experimental Design of Electrocoagulation and Magnetic Technology for Enhancing Suspended Solids Removal from Synthetic Wastewater," *International Journal of Science and Engineering*, vol. 7, no. 2, pp. 178-192, 2014.
- [81] S. S. Hamdan and M. H. El-Naas, "An electrocoagulation column (ECC) for groundwater purification," *Journal of Water Process Engineering*, vol. 4, pp. 25-30, 12// 2014.
- [82] M. Kobya, F. Ozyonar, E. Demirbas, E. Sik, and M. S. Oncel, "Arsenic removal from groundwater of Sivas-Şarkışla Plain, Turkey by electrocoagulation process: Comparing with iron plate and ball electrodes," *Journal of Environmental Chemical Engineering*, vol. 3, no. 2, pp. 1096-1106, 6// 2015.
- [83] E. S. Z. El-Ashtoukhy, N. K. Amin, and O. Abdelwahab, "Treatment of paper mill effluents in a batch-stirred electrochemical tank reactor," *Chemical Engineering Journal*, vol. 146, no. 2, pp. 205-210, 2/1/ 2009.
- [84] E. El-Ashtoukhy, Y. El-Taweel, O. Abdelwahab, and E. Nassef, "Treatment of petrochemical wastewater containing phenolic compounds by electrocoagulation

- using a fixed bed electrochemical reactor," *Int. J. Electrochem. Sci*, vol. 8, no. 1, pp. 1534-1550, 2013.
- [85] R. Chaudhary and O. P. Sahu, "Treatment of Sugar Waste Water by Electrocoagulation," *Journal of Atmospheric Pollution*, vol. 1, no. 1, pp. 5-7, 2013.
- [86] N. Vivek Narayanan and M. Ganesan, "Use of adsorption using granular activated carbon (GAC) for the enhancement of removal of chromium from synthetic wastewater by electrocoagulation," *Journal of Hazardous Materials*, vol. 161, no. 1, pp. 575-580, 1/15/ 2009.
- [87] Y. Mountassir, A. Benyaich, P. Berçot, and M. Rezrazi, "Potential use of clay in electrocoagulation process of textile wastewater: Treatment performance and flocs characterization," *Journal of Environmental Chemical Engineering*, vol. 3, no. 4, Part A, pp. 2900-2908, 12// 2015.
- [88] O. T. Can, M. Kobya, E. Demirbas, and M. Bayramoglu, "Treatment of the textile wastewater by combined electrocoagulation," *Chemosphere*, vol. 62, no. 2, pp. 181-187, 1// 2006.
- [89] (15<sup>th</sup> March 15<sup>th</sup> March). *F&T water solutions*. Available: <http://www.ftwatersolutions.com/electrocoagulation/variable-electro-precipitator>
- [90] (22<sup>nd</sup> February 22<sup>nd</sup> February). *Natural systems, environmental technology services*. Available: <http://www.n-systems.net/case3.htm>
- [91] M. Bayramoglu, M. Eyvaz, and M. Kobya, "Treatment of the textile wastewater by electrocoagulation: Economical evaluation," *Chemical Engineering Journal*, vol. 128, no. 2–3, pp. 155-161, 4/1/ 2007.

- [92] J. Rodriguez, S. Stopić, G. Krause, and B. Friedrich, "Feasibility assessment of electrocoagulation towards a new sustainable wastewater treatment," *Environmental Science and Pollution Research - International*, journal article vol. 14, no. 7, pp. 477-482, 2007.
- [93] C.-J. Lin, S.-L. Lo, C.-Y. Kuo, and C.-H. Wu, "Pilot-Scale Electrocoagulation with Bipolar Aluminum Electrodes for On-Site Domestic Greywater Reuse," *Journal of Environmental Engineering*, vol. 131, no. 3, pp. 491-495, 2005.
- [94] M. Nasiri and I. Jafari, "Produced Water from Oil-Gas Plants: A Short Review on Challenges and Opportunities," *Periodica Polytechnica Chemical Engineering*, 2016.
- [95] J. A. Ahan, "CHARACTERIZATION OF PRODUCED WATER FROM TWO OFFSHORE OIL FIELDS IN QATAR," QATAR UNIVERSITY, 2014.
- [96] J. Veil, M. Puder, D. Elcock, and R. Redweik Jr, "A white paper describing produced water from production of crude oil, natural gas and coal bed methane. Argonne National Laboratory," *Contract W-31-109-Eng-38*, 2004.
- [97] J. D. Arthur, B. G. Langhus, and C. Patel, "Technical summary of oil & gas produced water treatment technologies," *All Consulting, LLC, Tulsa, OK*, 2005.
- [98] P. Jain, M. Sharma, P. Dureja, P. M. Sarma, and B. Lal, "Bioelectrochemical approaches for removal of sulfate, hydrocarbon and salinity from produced water," *Chemosphere*, vol. 166, pp. 96-108, 1// 2017.
- [99] A. Fakhru'l-Razi, A. Pendashteh, L. C. Abdullah, D. R. A. Biak, S. S. Madaeni, and Z. Z. Abidin, "Review of technologies for oil and gas produced water treatment," *Journal of hazardous materials*, vol. 170, no. 2, pp. 530-551, 2009.

- [100] J. A. Veil, M. G. Puder, D. Elcock, and R. J. Redweik Jr, "A white paper describing produced water from production of crude oil, natural gas, and coal bed methane," *Argonne National Laboratory, Technical Report*, 2004.
- [101] J. Veil, "Why are produced water discharge standards different throughout the world," *Environmental Science Division Argonne National Laboratory. 13th IPEC, San Antonio, Texas, October 19th. [ipcc.utulsa.edu/Conf2006/Papers/Veil/prodwater.pdf](http://ipcc.utulsa.edu/Conf2006/Papers/Veil/prodwater.pdf)*, 2006.
- [102] R. Bernier *et al.*, "Environmental aspects of the use and disposal of non aqueous drilling fluids associated with offshore oil & gas operations," *International Association of Oil & Gas Producers Report*, vol. 342, 2003.
- [103] H. Backer *et al.*, "HELCOM Baltic Sea Action Plan—A regional programme of measures for the marine environment based on the Ecosystem Approach," *Marine pollution bulletin*, vol. 60, no. 5, pp. 642-649, 2010.
- [104] N. Gaurina-Medimurec, K. Simon, and B. Pašić, "Offshore Drilling and Environmental Protection," in *Energy and Environment (Energija i okoliš) 2006*, 2006.
- [105] N. Esmaeilrad, K. Carlson, and P. Omur Ozbek, "Influence of softening sequencing on electrocoagulation treatment of produced water," *Journal of Hazardous Materials*, vol. 283, pp. 721-729, 2/11/ 2015.
- [106] F. L. Lobo, H. Wang, T. Huggins, J. Rosenblum, K. G. Linden, and Z. J. Ren, "Low-energy hydraulic fracturing wastewater treatment via AC powered electrocoagulation with biochar," *Journal of Hazardous Materials*, vol. 309, pp. 180-184, 5/15/ 2016.



- [107] J. Gomes, D. Cocke, K. Das, M. Guttula, D. Tran, and J. Beckman, "Treatment of produced water by electrocoagulation," 2009.
- [108] S. Zhao, G. Huang, G. Cheng, Y. Wang, and H. Fu, "Hardness, COD and turbidity removals from produced water by electrocoagulation pretreatment prior to Reverse Osmosis membranes," *Desalination*, vol. 344, pp. 454-462, 7/1/ 2014.
- [109] S. H. Ammar and A. S. Akbar, "Oilfield produced water treatment in internal-loop airlift reactor using electrocoagulation/flotation technique," *Chinese Journal of Chemical Engineering*, 2017/08/04/ 2017.
- [110] E. H. Ezechi, M. H. Isa, S. R. M. Kutty, and A. Yaqub, "Boron removal from produced water using electrocoagulation," *Process Safety and Environmental Protection*, vol. 92, no. 6, pp. 509-514, 11// 2014.